CHALMERS
UNIVERSITY OF TECHNOLOGY


# Aerodynamics Concept Study of Electric Vehicles

Drag Reduction and Range Increase

Master's Thesis in Automotive Engineering

Umut Aktaş
Kristian Abdallah

Department of Applied Mechanics
CHALMERS UNIVERSITY OF TECHNOLOGY
Gothenburg, Sweden 2017

Master's thesis 2017:33

# Aerodynamics Concept Study of Electric Vehicles

Drag Reduction and Range Increase

UMUT AKTAŞ
KRISTIAN ABDALLAH

Department of Applied Mechanics
*Division of Vehicle Engineering and Autonomous Systems*
Chalmers University of Technology
Gothenburg, Sweden 2017

Aerodynamics Concept Study of Electric Vehicles
Drag Reduction and Range Increase
UMUT AKTAŞ, KRISTIAN ABDALLAH



Supervisor: Mohammad El-Alti, NEVS AB
Examiner: Simone Sebben, Chalmers University of Technology

Master's Thesis 2017:33
Department of Applied Mechanics
Division of Vehicle Engineering and Autonomous Systems
Chalmers University of Technology
SE-412 96 Gothenburg
Telephone +46 31 772 1000

Cover: NEVS 9-3 Concept Vehicle

Chalmers Reproservice
Gothenburg, Sweden 2017

Aerodynamics Concept Study of Electric Vehicles
Drag Reduction and Range Increase
UMUT AKTAŞ, KRISTIAN ABDALLAH
Department of Applied Mechanics
Chalmers University of Technology

# Abstract

As the greenhouse effect is causing climate instability all over the world, this issue must be adressed. One of the main contributor to this is the transportation sector which have been using fossil fuels to fire up the engines. Car manufacturers are today taken this issue in consideration and are starting to implement a more sustainable approach when developing and building new vehicles.

NEVS is one of the car companies that have taken a major step towards creating a sustainable future. The approach is to develop pure electric vehicles and fleet sharing services driven by renewable sources which would contribute to a significant reduction of greenhouse gases.

With the air resistance exerted on a driven vehicle being the largest energy consuming attribut, this thesis is done in collaboration with NEVS to study different approaches to reduce the aerodynamic drag. The study is divided into two parts, a theoretical part where a benchmarking study and a literature review is done and a practical part where concepts based on the theoretical part are chosen to be analyzed with CFD simulations. The simulation environment represents a highway drive where the aerodynamic energy loss is the highest.

The simulated concepts resulted in drag reductions of up to 4% for the best cases. These cases corresponds to active aerodynamic features and is used in order to delay the separation at the rear-end of a vehicle.

To conclude the study, it is shown that the aerodynamic performance of today's vehicles have not yet reached its fully potential. As different concepts are analyzed it is found that with the use of aerodynamic features the drag can significantly be reduced hence increasing the range of electrical vehicles.

Keywords: Electric Concept Vehicle, DrivAer Model, Aerodynamics, Drag Coefficient, Air Curtain, Wheelhouse Ventilation, Front Spoiler, Underbody Vanes, Diffuser Extension, Roof and Trunk Spoiler Extension

# Acknowledgements

This thesis is done as a final step in order to obtain a Master of Science Degree in Automotive Engineering. It is performed at NEVS in Trollhättan within the CFD and thermal CAE department.

During our time at NEVS, by working on this thesis and interacting with the company workers, we have gained a lot of knowledge in the electric vehicle market and its progressions. With that, we would like to express our biggest gratitudes to Mohammad El-Alti, Lead Engineer CFD and Thermal CAE at NEVS for giving us the opportunity to collaborate with NEVS and also for his support and guidance along this thesis. Also we want to give special thanks to the rest of the CFD Team at NEVS for their major support.

A special thanks is to Prof.Simone Sebben, Head of Vehicle Engineering and Autonomous Systems at Chalmers as she have taught us everything we know about vehicle aerodynamics. With her experience and wide knowledge in this field, Simone have been a great tutor during our time at Chalmers and throughout this thesis.

Finally, we would like to thank the silent heroes, our families and friends for their support and their belief in us.

Gothenburg, 5 June 2017

Umut Aktaş  Kristian Abdallah

# Contents

# List of Figures

# List of Tables

# 1

# Introduction

## 1.1 Project Background

There are no denials that the greenhouse effect have resulted in an increase of temperatures all over the world. This effect is accelerating the ice meltings in the Arctic Sea which consequently are resulting in the rise of water levels. Additionally, the increase of temperatures along the equator line are resulting in dryer areas and hence a size increase of the deserts.

Some of the main contributors to the greenhouse effect are the burning of fossil fuels for transportation and heating and land clearing in order to create buildings to the increasing population. In cities such as Beijing, Paris and London the air pollution is today reaching so high levels that it is posing a threat on the public health. These governing issues are making governments all over the world constantly creating and updating climate policies.

The transport sector is currently the main consumer of fossil fuels in form of gasoline and diesel. The consumption in Europe corresponds to 33% of the total consumption (Eurostad, 2015),thus addressing the importance of increasing the efficiency and lowering the energy losses of the vehicles sold in the market. Car manufacturers are starting to implement a more sustainable approach when developing vehicles with the focus on electrification or hybrid solutions in order to reduce and/or eliminate the use of fossil fuels.

As the drivetrain of the vehicles are getting more efficient, other contributors to significant energy losses are appearing. According to Barnard (Barnard, 2009), a significant contribution to the energy consumption of vehicles comes from the air resistance that a vehicle is exerted to. For an electric vehicle, the air resistance can reach up to 48% of the total driving resistance at highway speeds.(Lohse-Busch et al., 2013)

The main gain in reducing the air resistance by improving the aerodynamics of an electric vehicle is the increase of range that a vehicle can travel. In a study made by Tesla Inc., it is shown that a 10% improvement of the aerodynamic performance can result in a 5% increase of range.(Palin et al, 2012)

## 1.2 Company Background

Founded in April 2012, NEVS AB (National Electric Vehicle Sweden) is a car company focusing on the development and production of premium electric vehicles together with mobility, connectivity and automation.

NEVS acquired the assets of the former car company SAAB Automobiles AB from a bankruptcy in 2012 and has since then worked towards their vision to develop mobility solutions to shape a more sustainable future. The mobility solution makes it possible to travel anywhere, anytime using a fleet sharing service which eliminates the need of buying and owning a vehicle. Together with that, the focus on pure electric vehicles and automated driving removes the need for driving which gives the customer free personal time while using the service.

The company has two R&D centers with production facilities, one in Trollhättan Sweden and one in Tianjin China with a total production capacity of 380 000 cars per year. Another recent agreement has granted NEVS a third production plant in the Fujian province in China. (NEVS, 2015)

The main owner of NEVS is Kai Johan Jiang. Mr. Jiang is a pioneer within the bio energy industry and with his Hongkong based company, National Modern Energy Holdings, he in collaboration with his co-workers builds and runs power plants. A belief in renewable energy as a profitable venture and a more sustainable future has been the driving force throughout his career.

## 1.3 Project Description

The air resistance of an electric vehicle is with no doubt one of the largest energy consuming vehicle attribute. In the automotive industry, concept vehicles with great aerodynamic performances are continuously studied in order to gain knowledge in flow characteristics and flow behaviour when interacting with a vehicle geometry. It is shown that streamlined vehicles from different car manufacturers have common features to control and guide the flow in order to reduce the air resistance and hence improve the aerodynamic performance. The key for success is both to manage the flow and to keep the car functional and attractive.

### Purpose

This master thesis combines a thorough study of the development of historical, current and futuristic aerodynamics concept vehicles with a quantified CFD analysis where selected features are studied. The purpose is to provide NEVS with features and/or functions that benefits the company in the work with improving the aerodynamic performance and hence increasing the range of their vehicles.

## Objectives

The objectives of the thesis are

- Benchmarking of historical, current and futuristic aerodynamics concept vehicles
- CFD simulations together with analyses in order to give suggestions for an improved aerodynamic performance

## Limitations

The area of aerodynamic is large and for a thesis work it is needed some limitations which are listed below

- The benchmarking is only based on both conceptual and actual vehicles that have impacted the history of vehicle aerodynamics.
- The study is focusing on reducing the drag coefficient and is not considering how the lift coefficient is affected.
- The designed features do not have an optimized geometry thus a thorough study is needed for each feature in order to give the best performance
- Computational time is valued higher than an accurate drag coefficient value.
- Focus is on drag coefficient changes and trends between the concepts
- Only the fastback and estateback configurations of the DrivAer Model are used

# 2

# Benchmarking

## 2.1 Historic Development of Vehicle Aerodynamics

The 1920's set the date when the aspect of the aerodynamics and its influence on vehicle design was started to be investigated in. Vehicles with streamlined designs started to take over the roads and with compromises to the exterior design of the vehicles, the drag coefficient (Cd) which is a dimensionless number that is used to compare the aerodynamic performance of vehicles, was significantly decreased.

The streamlined designs that started to become more and more usual in vehicle designs originated in the aircraft and airship industry. One engineer, named Jaray worked for a Zeppelin airship company and came to be a pioneer in automotive streamlining. Jaray worked with the aerodynamics of airships and spend a lot of time in the windtunnel. His aerodynamic discoveries were followed by investigations of aerodynamics in passenger vehicles.(Marti, 1931 and Brown et al., 1934) In 1922, Jaray and his colleague Klemperer studied how simple bodies and the proximity to a ground surface influenced their aerodynamic performance. Their findings showed that a "half-body" teardrop shape with wheels results in a Cd value of 0.15 which is 20-25% less than of the passenger cars of today.(Hucho, 1998) In figure 2.1, the studied bodies and their coherence to Cd values are shown.

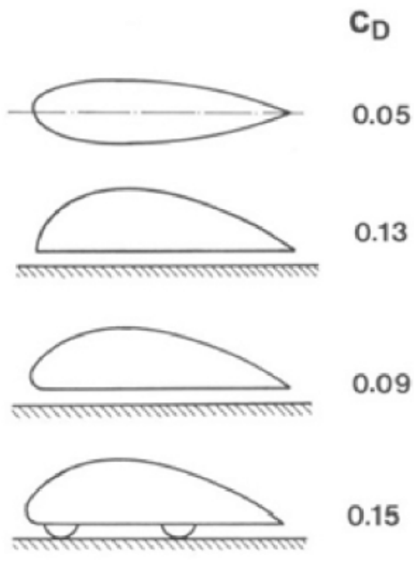


**Figure 2.1:** Test results of Jaray's and Klemperer's study (Good et al, 2011)

Based on the results, Jaray decided to use his experience in the aerodynamic field and started to design vehicles with focus of aerodynamics. One of his most famous work was the Tatra T77 which is shown in figure 2.2. The Tatra T77 became the car with the lowest drag coefficient in the 1920s with a Cd value of 0.21. (Good et al., 2011)

**Figure 2.2:** Tatra T77 designed by Jaray.(Google Img. Library)

Jaray succeded and based on public acceptance to aerodynamics, car manufacturers such as Fiat, Maybach and Audi decided to collaborate with him in order to implement aerodynamics in some of their vehicle designs. In Figure 2.3, different vehicles designed by Jaray are shown.

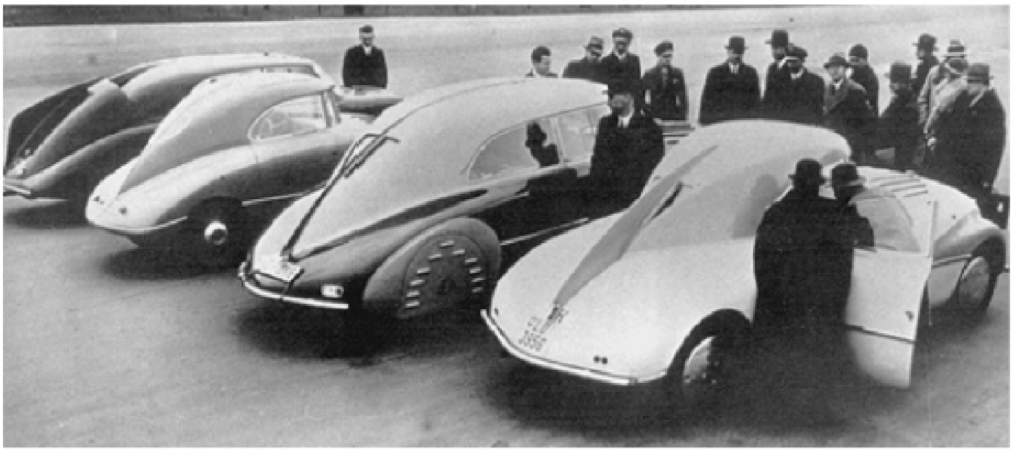

**Figure 2.3:** Jaray's designs for (Left to Right): Tatra, Fiat Balilla, Maybach and Audi. (Google Img. Library)

One disadvantage with Jaray's design was that the space for rear passengers was very limited. This opened up for other car manufacturers to deliver streamlined vehicles with enough spacing. One of the first car companies to do this was Chrysler who started their wind tunnel tests in the late 1920s. The result was a vehicle design with a Cd value of 0.56 which encountered 30% less wind resistance compared to their origin way of designing vehicles. This car was named Chrysler Airflow Coupé, shown in figure 2.4 and was launched at the 1934 Motor Show in New York. (Breer et al, 1995)

**Figure 2.4:** 1934 Chrysler Airflow Coupé (Google Img. Library)

Parallel with Jarray, an aeronautical engineer named Sir Charles Dennistoun Burney caught interest in automotive streamlining and started his investigations in the late 1920's. Sir Charles gained success and by 1927, thirteen versions of his design concepts were built. Sir Burney's concept cars were different than the typical production cars of today. One significant difference was the characteristics of the body which could reach lengths of up to 6 meters. Placing the engine in the rear-end of the vehicle, the front-end was reduced to a tiny overhang where as the rear-end had a long overhang, as shown in figure 2.5. This way of designing vehicles was at that time eye-catching. Sir Charles collaborated with Crossley Motors, who built the streamlined cars.(Good et al, 2011)

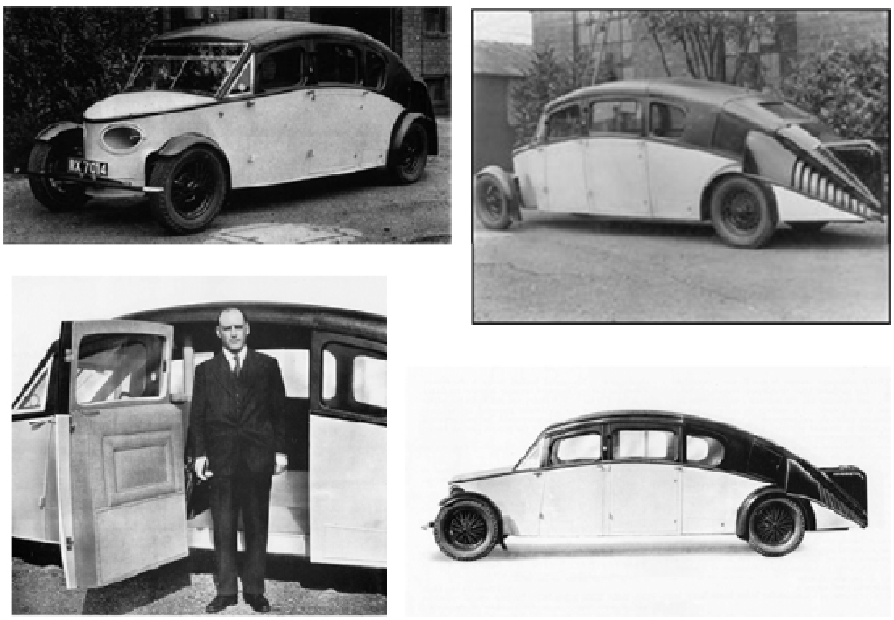

**Figure 2.5:** Burney's streamlined vehicles (Good et al, 2011)

In an aerodynamic aspect, the enhancements of the Sir Burney's vehicles in terms of aerodynamic performance was the shape of the front sides, the roof curvature and the underbody which was covered by sheet metal. Disadvantages are, even though a tiny front-end was used, that 60% of the contribution to drag comes from the nose, screen and front wheels. Overall, with all these features, the Cd value of Sir Charles's streamlined vehicle design was approximately 50% higher than a typical competitor vehicles at that time.(Good et al, 2011)

In the late 1930s, as car manufacturers still were gaining knowledge in automotive streamlining, European and American car manufacturers were building their new vehicles with some key features. This features included a curvaceous body, a tapered tail, wheelhousing within the main body and a sloped windscreen. Figure 2.6 shows one of the models, Lincoln Zephyr, that was inspired by Chrysler Airflow but with an improved aerodynamic performance resulted in a Cd value of 0.45. Throughout the 1940s and 1950s, the same design language was used for production vehicles due to World War II.(Good et al, 2011)

**Figure 2.6:** 1936 Lincoln Zephyr (Good et al, 2011)

The aerodynamic development of the vehicles continued after World War II. The Italian car manufacturer Fiat released a concept vehicle named Fiat Turbina with a Cd value of 0.14, shown in figure 2.7. The vehicle was developed for high-end performance and uses a jet engine instead of a conventional internal combustion engine. This configuration benefited the designers whom put effort on the aerodynamics and designed the vehicle according to that. As a result, the Fiat Turbina is a vehicle which have held the record for having the lowest drag coefficient in the automotive world for 30 years and still counting.(Hemmings, 2006)

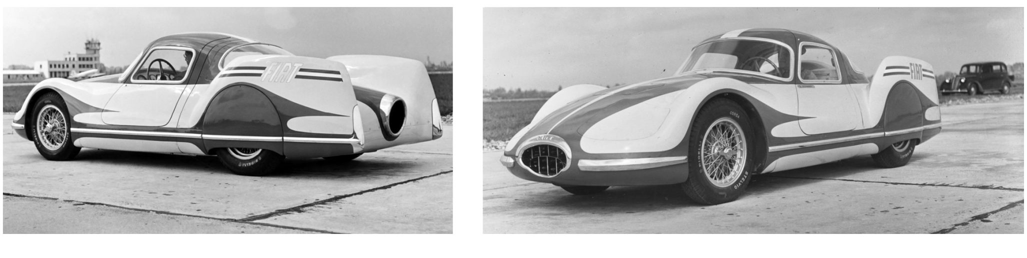

**Figure 2.7:** 1954 Fiat Turbina (Google Img. Library)

Meantime in the late 1950s, another Italian car manufacturer, Alfa Romeo built and released three concept vehicles shown in figure 2.8. The first vehicle, BAT 5 was unveiled at 1953 with a Cd value of 0.23 followed by the BAT 7 and BAT 9 models which both have a Cd value of 0.19. The streamlined design of the vehicles is completed with the huge tail fins and their curvature which at that time was a signature feature for Alfa Romeo.

**Figure 2.8:** 1956 Alfa Romeo BAT vehicles (L to R: BAT 5, BAT 7, BAT 9) (Google Img. Library)

According to the study made by Good (Good et al, 2011), after 1960 many car manufacturers started basing their aerodynamic design on Hucho's studies.(Hucho et al, 1976 and Buchheim, 1981) Hucho's investigations provided the car manufacturers approaches to optimize their current vehicle design in order to further improve their aerodynamic performance. Based on these approaches, some researchers such as Ahmed, Glihaus and Renn, Carr and Howell have studied and published generic data which has been guiding the automotive streamlining for a long time period.

Based on these studies the German car manufacturer, Audi AG, developed a car in 1983 called Audi 100 and was designed by Buchheim. The car was claimed to have the lowest drag coefficient for a production car of that time with a Cd value of 0.30. The car is shown in figure 2.9.(Buchheim, 1982)

**Figure 2.9:** 1983 Audi 100 Sedan (Google Img. Library)

Six years after the Audi 100 was launched, another German car manufacturer, Opel reveals the Opel Calibra shown in figure 2.10. The Opel Calibra was designed by Emmelmann and had a Cd value of 0.26 which made it the vehicle with the lowest drag coefficient in the market.(Emmelmann, 1990)


**Figure 2.10:** 1989 Opel Calibra Coupe (Google Img. Library)

During and after the 1990s, car manufacturers started turning towards looking for alternative types of powertrains to replace the internal combustion engine due to air pollution and increasing oil prices. The most ideal idea was the electrification of the vehicle. However, the capacity of the battery, which at that time wasn't as developed and long-lived as today, was a huge problem. To work around this problem, the internal combustion engine was made smaller and combined with electric motors to create hybrids. With this, the efficiency of the powertrains increased and resulted in increasing effort and focus on the aerodynamic performance of the vehicles due to its impact on saving fuel and increasing the range of the electric battery.

As a result of this, the American car manufacturer, General Motors, released the EV1 in 1996. The EV1 was a pure electric driven vehicle with a Cd value of 0.19. (Larminie, 2003) A significant contribution to the low Cd value was that the EV1 had except of the streamlined design, a complete closed front and covered rear wheelhouses as seen in 2.11. These features results in a more than 10% reduction of the Cd compared to the traditional conventional vehicles, which have a cooling package placed in the front-end and thus needs to keep the front open.(Hucho, 1998)

**Figure 2.11:** 1996 Genaral Motors EV1 (Google Img. Library)

In the same time the aerodynamic performance of the conventional vehicles was still developed and improved by aerodynamic engineers. In 1999, Honda released the Insight and in 2001 Audi released the A2, shown in figure 2.12. Both vehicle models had a Cd value of 0.25 making them sharing the first place as the conventional vehicles with the lowest drag coefficient in the market, pushing the Opel Calibra down from the lead.(Audi, 1999) (Broke, 2010)

**Figure 2.12:** 1999 Honda Insight(Left), 2001 Audi A2(Right)(Google Library)

Despite the fact that the Honda Insight and the Audi A2 was the lowest drag coefficient vehicles, they did not satisfy the customer demands due to them being sold in the mini car segment.

With improved windtunnel setups and increased computational resources, car manufacturers was given new and better tools to improve testing and as a result the aerodynamic performance could further be enhanced. One big setback however, that limited the possibility to design a fully streamlined vehicle was the progression of government regulations and legislation on safety, comfort and functionality.

With all this going on, the German car manufacturer, BMW, released in the end of 2004 the 3 Series Sedan as shown in figure 2.13. With a Cd value of 0.26 this vehicle fulfilled not only all regulations and legislations but also met the customer demands as it had room for passengers and a larger trunk section for storage compared to the Honda Insight and Audi A2. This with only 0.01 difference in Cd.(Good et al, 2011)

**Figure 2.13:** 2005 BMW 3 Series Sedan (Google Img. Library)

In 1997, the Japanese car manufacturer Toyota, released a hybrid vehicle which came to surprise the world and is still one of the worlds most sold hybrid vehicle.

The vehicle was named the Prius and is shown in figure 2.14. Due to the vehicle being a hybrid it was a big hit for customers caring about the greenhouse effect and its reduction. In 2006, the 3rd generation Prius was released and with an aerodynamically improvement resulting in a Cd value of 0.25. (Broke, 2010)

**Figure 2.14:** 2006 Toyota Prius, 3rd Generation (Google Img. Library)

To summarize the historcal development of vehicle aerodynamics, the car manufacturers have continuously worked towards reducing the Cd value of their vehicles. As shown in figure 2.15, the reduction of Cd is rapidly decreased from 1920s until today. As more and more effort is put on increasing efficiency of the vehicles and reducing the energy losses, more and more focus is put on the aerodynamic performance due to it contributing to a significant part of the energy losses.

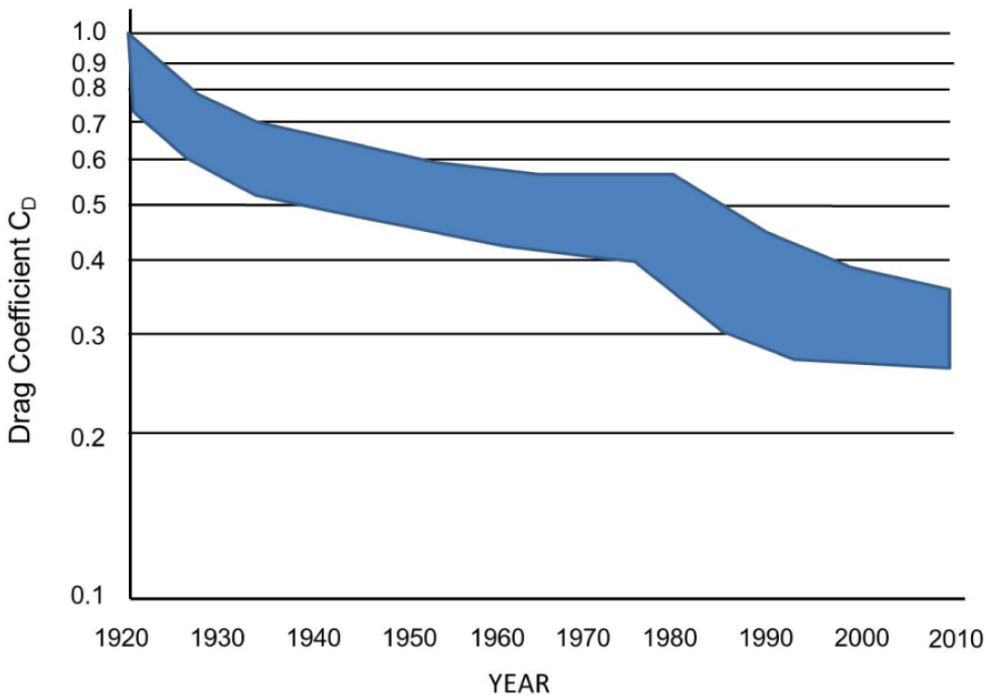


**Figure 2.15:** The reduction of Cd values from the 1920s until today. (Good et al, 2011)

## 2.2 Current Development of Vehicle Aerodynamics

As safety, comfort and functionality requirements together with governmental regulations and legislations results in setbacks when considering the the aerodynamic aspect, car manufacturers are continuously finding ways to work towards more aerodynamically developed vehicles. Additonal to that, with new technologies new type of features such as active aerodynamic features are being used. An active aerodynamic feature is a function that is only enabled when needed e.g during a highway drive. A passive feature is a function that is constantly enabled e.g a front grille that is used to cool the engine coolant for conventional vehicles. Vehicle design is included in the passive aerodynamic section and as seen in the historical development of aerodynamics, this was the main area of study in order to reduce the drag coefficient.

In 2013, Mercedes-Benz released the lowest drag coefficient vehicle in the market. The vehicle was named CLA, presented in figure 2.16, and had a Cd value of 0.23. This vehicle used both passive and active aerodynamic features.(Daimler AG, 2017) The main active feature of his vehicle is the active grille shutter system. This system uses flaps in the front grille that turns into a closed state when enabled which could be when the engine and brakes does not need to be cooled. A 10% drag coefficient decrease can be obtained with this function as mentioned for the EV1 car (figure 2.11). Additional to that, Mercedes CLA has aerodynamically optimized side mirror housings, improved A-pillar curvature, well design rear-end design and a diffuser at the end of the underbody.

**Figure 2.16:** 2013 Mercedes CLA (Google Img. Library)

In 2016, the American electric car manufacturer Tesla INC introduced a facelift on their flagship model the Model S shown in figure 2.17. The vehicle has a Cd value of 0.24 and uses aerodynamic features such as a closed front due to the fact that electric vehicles do not require as much cooling as for conventional vehicles, air curtains located in the front bumper to direct the airflow past the front tires and a flat underbody panel to reduce the airflow disturbance along the underbody. The passive aerodynamic features are aerodynamic wheel rims, hidden door handles and floating C-pillars which is developed to reduce the wake behind of the vehicle. (Tesla INC, 2017)

**Figure 2.17:** 2016 Tesla Model S (Tesla INC, 2017)

At the same time as the facelift of the model S, Tesla introduced the Model X which is the first pure electric SUV ever to be sold in the market. The Tesla Model X has the same aerodynamic features as Model S, however the only difference is the rear roof spoiler that is used to provide an increase in downforce at the rear-end of the vehicle at higher speeds. Compared to a conventional SUV, the Model X have a sportive aesthetic rear as shown in figure 2.18.

**Figure 2.18:** 2016 Tesla Model X (Tesla INC, 2017)

In 2017, the vehicle with the current lowest drag coefficient was released by BMW. It is the new 5 Series Sedan shown in figure 2.19. The 5 Series have a Cd value of 0.22 and as its other aerodynamically competitive vehicles the BMW uses both active and passive aerodynamic features in order to reduce the drag coefficient.(BMW AG, 2017) These features are again the active front grille shutter, large areas of underbody panelling with additional covers in the rear axle area, air curtains at front end, front wheelhouse ventilations and aerodynamic wheel rims.


**Figure 2.19:** 2017 BMW 5 Series Sedan (BMW AG, 2017)

## 2.3 Futuristic Development of Vehicle Aerodynamics

A vehicle conceptual design gives an insight in the futuristic development and inspires car manufacturers. Furthermore it gives ideas to designers for to create new design languages eras. Since the concept vehicles are not sold in the market there are no limitations in form of regulations and legislations giving the designers free hands to expand their creativity. As a result, highly streamlined vehicles with exceptional aerodynamic performance can be created.

In 2011, Volkswagen revealed the XL1 Super efficient vehicle with a Cd value of 0.19.(Volkswagen AG, 2017) The XL1 is holding the record for the lowest drag coefficient concept vehicle in the 2010s. From the design, shown in figure 2.20 the first prominence is that the side mirrors are replaced with cameras. Removing the side mirror does not only influence the drag coefficient but also reduces the frontal area. Additional to that the rear wheelhouses are covered, a closed front and a floating c-pillar are used.

**Figure 2.20:** 2011 Volkswagen XL1 Super Efficient Vehicle (Volkswagen AG, 2017)

In the 2015 Frankfurt Motor Show, several vehicle manufacturers such as Mercedes-Benz and Audi revealed their concept vehicles that employ active aerodynamic features and other designs and functions in order to reduce drag. Mercedes-Benz presented the Concept Intelligent Aerodynamic Automobile(Concept IAA) shown in figure 2.21. At around 80 km/h, with several active aerodynamic features, the vehicle switches from regular to aerodynamic mode. At the rear-end, an extension extends by up to 390 mm in order to reduce the wake. The spoiler in the lower part of the front bumper folds down by 60 mm to improve the flow along the underbody. Flaps in side parts of the front bumper extends outwards by 25 mm and move back by 200 mm for an improvement of the airflow past the front wheel arches. With all the active features enabled, the drag coefficient drops from 0.25 to 0.19.(Gehm, 2015) Additional to that, the IAA concept uses cameras instead of the traditional side mirrors, no door handles and huge wheelhouse ventilations for an improved aerodynamic performance.

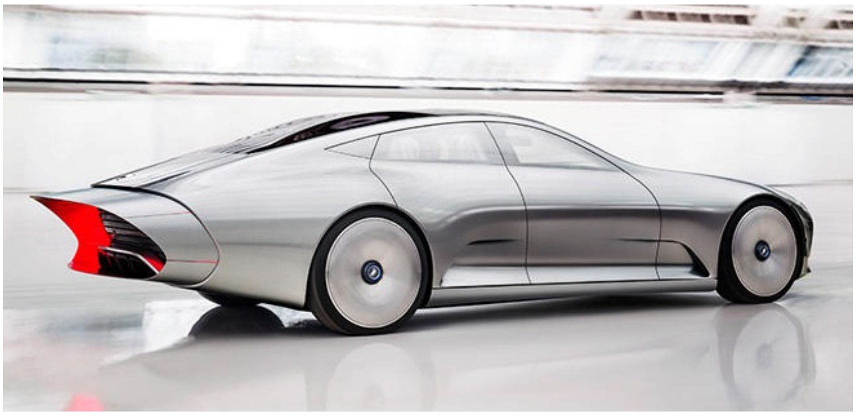

**Figure 2.21:** 2015 Mercedes IAA Concept Vehicle (Daimler AG, 2015)

In the same motor show, Audi revealed their concept SUV model called the e-tron Quattro Concept shown in figure 2.22. According to Audi, the e-tron Quattro Concept has a range of more than 500 km with the help of active aerodynamic features which gives the vehicle a Cd value of 0.25 hence becoming the best in the segment. Same as for the Mercedes IAA concept, all the aerodynamic features are being enabled after a vehicle speed of 80 km/h. The active roof spoiler of the vehicle extends by 100 mm to delay the separation at rear and hence reduce the wake. The same time as the roof spoiler extends at the top, the active diffuser extends 100 mm from the lower rear-end of the vehicle. Additional to that, side sills are extended outwards by 50 mm to direct the airflow past the rear wheels.(Gehm, 2015)

**Figure 2.22:** 2015 Audi e-tron Quattro Concept (Google Img. Libarary)

## 2.4 Aerodynamic Features

Ever since the 1920s, which started the era of automotive streamlining a continuous work towards improving the aerodynamic performance of vehicles is done. The traditional way of improving the vehicle aerodynamics has been by optimizing the vehicle geometry and surface. However with government regulations and legislations and also the need to fulfill the customer demands, the possibility to create a completely aerodynamic vehicle design is limited. Car manufacturers adjusts to the limitations and continuously find other innovative ways to improve the aerodynamic performance which fulfills all criterion.

By using aerodynamic features, the aerodynamic performance is improved without, in many cases, clashing with the regulations and legislations. These features are traditionally passive which means that they are always in operation. With new technologies and cheaper electronic components, active aerodynamic features are growing. An active feature is manually or automatically enabled and disabled when not needed, e.g. an extendable roof spoiler.

In table 2.1, passive and active features that have been discovered in this benchmarking study are listed.

**Table 2.1:** Aerodynamic features discovered in the benchmarking study.

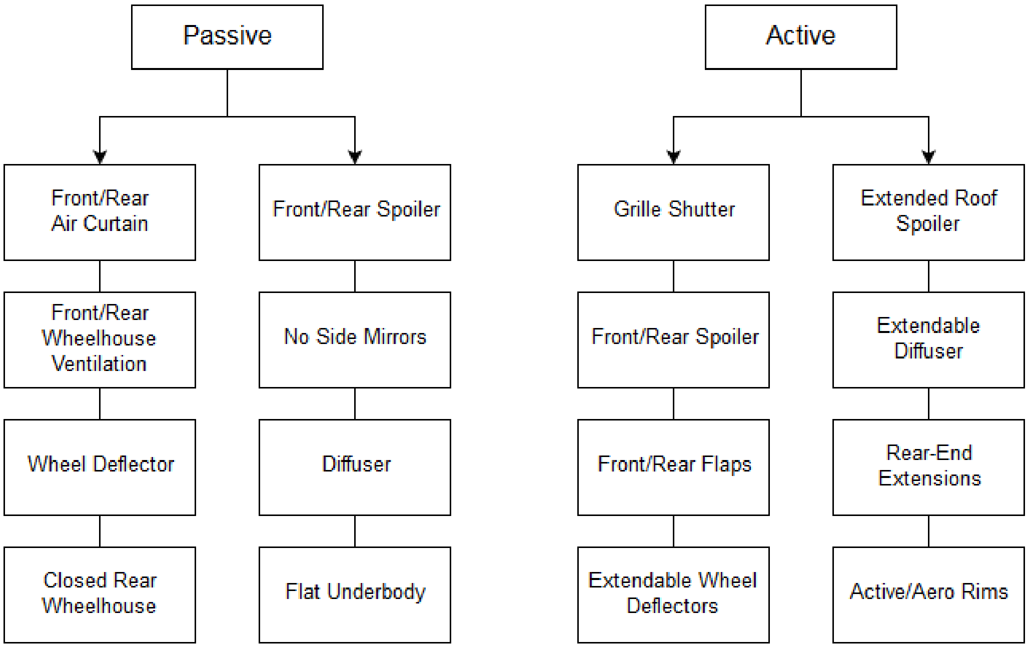


This list presents aerodynamic features that are located all over a vehicle body. A literature review study in which the design parameters and the contribution to drag for different vehicle designs and features is presented in the following chapter.

# 3

# Literature Study

## 3.1 Aerodynamics of Passenger Vehicles

A vehicle have a very complex geometry in the aspects of aerodynamics. The need of cooling heated parts and the influence of rotating wheels requires a highly efficient way of controlling the airflow, which is interacting with the vehicle. In order to understand where the air resistance is created and how much is contributing to drag, many investigations have been made. In figure 3.1, the sectioning of a passenger vehicle corresponding to the contribution of drag according to Sebben (Sebben et al, 2016) is presented.

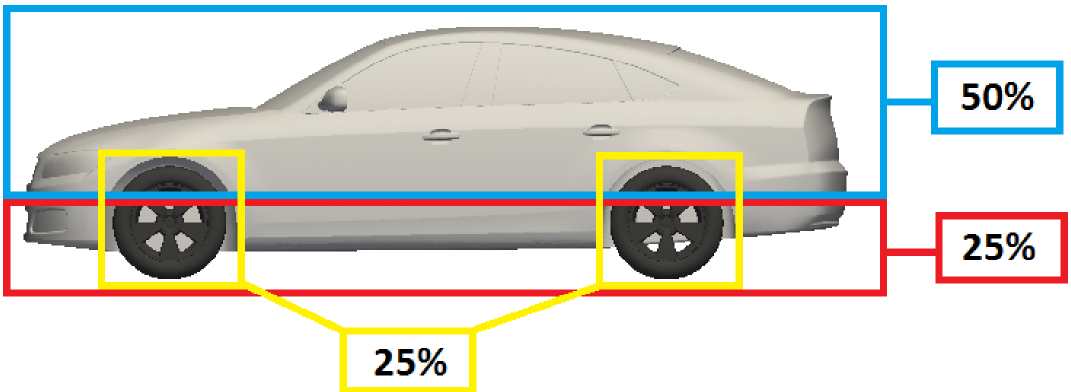


**Figure 3.1:** Drag contribution for a passenger vehicle.

In a typical passenger vehicle 50% of the drag is caused by the design of the upper-body including the upper parts of the front and rear-end. The wheels and wheel-houses correspond to 25% of the total drag and for conventional vehicles the same amount, 25%, arises from the underbody. In electric vehicles however, the use of a flat underbody panel allow the flow to freely pass along the underbody with no disturbances. This results in the lowering of the drag contribution that comes from the underbody resulting in the increase of the ratio in other areas.

Based on the benchmarking study, this chapter is divided into five different sections corresponding to different areas of a vehicle. All design languages and features found in the benchmarking are studied through literature studies. This is done to get an understanding on dimensions and placements of aerodynamic features and drag reducing trends.

### 3.1.1 Front-End

The front-end of a vehicle is where the first impact between the airflow and the vehicle is occuring, hence making the front-end design very important in order to control how the flow will behave along the rest of the vehicle. As a large stagnation area is created at the front-end and it corresponds to a major drag contribution, an improved front-end design would result in significant drag reductions. This is studied by Hucho (Hucho, 1998) where investigations in the effect of a front-end design on aerodynamics was made with several tests. In figure 3.2, the results are presented.

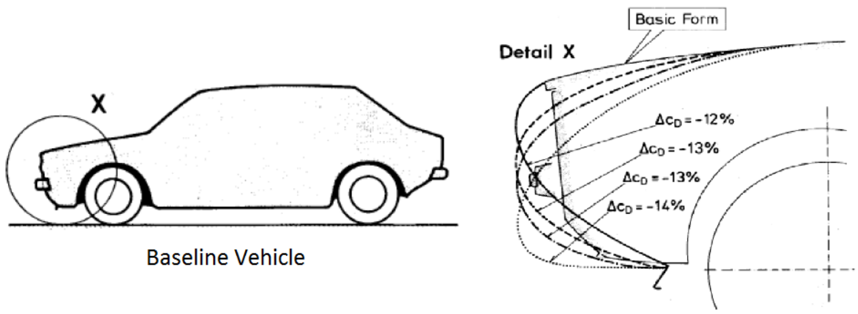


**Figure 3.2:** Front-end designs resulting in drag reductions.(Hucho, 1998)

Compared to the baseline model, Hucho could obtain up to 14% drag reduction by modifying the geometry of the front-end. The conclusion Hucho draw from this study was that by lowering the nose of the vehicle a gain in aerodynamic performance was obtained.

An aerodynamic feature correlating with the front-end design that was also studied by Hucho was the front spoiler. The front spoiler is used to reduce the front opening between the vehicle surface and the ground in order to reduce the airflow passing under the vehicle. This resulted in a smoother flow with an increased velocity thus lowering the pressure under the vehicle and hence increasing the downforce and also reducing drag. According to Hucho's continued studies of the front-end design, it is shown that using a spoiler with an optimal nose could reduce the total drag of a vehicle by 11-16%. This result is presented in figure 3.3.

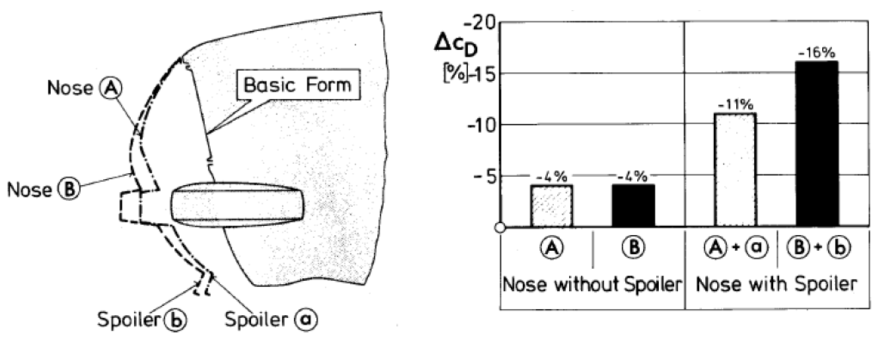


**Figure 3.3:** Front spoiler and its influence on drag reduction.(Hucho, 1998)

Another study of the front spoiler and its impact on the aerodynamic performance was made by Kumar. (Kumar et al, 2015) Kumar studied the influence of the front spoiler height and the clearance between the ground and the spoiler and found that a drag reduction of 1.5% could be obtained. With the addition of a splitter at the base of the front spoiler the drag can further be reduced by increased flow control. In a study made by Robinette (Robinette, 2016), different front spoiler and splitter designs were studied in order to reduce the drag of a conventional vehicle. Robinette found that a front spoiler/splitter combination resulted in a 20% drag reduction as shown in figure 3.4.


**Figure 3.4:** Drag coefficient for baseline vs spoiler/splitter. (Robinette, 2016)

The splitter feature allows for the flow to attach on the underside of the splitter early as the tip of the splitter is located ahead of the front of the vehicle. This results in a smoother airflow under the vehicle due to the splitter reduceing the separation occuring at the base edge of the front spoiler. The best spoiler/splitter combination had a ground clearance of 100mm and a 50mm wide splitter. With this type of feature, the frontal area of a vehicle is increased which is not desired in an aerodynamic aspect. This effect needs to be considered with the use of this feature.

### 3.1.2 Upper-Body

The upper-body of a vehicle do mainly consist of the so called greenhouse which includes the windshield, side windows, rear window, A- and C-pillars and the roofing. This section of the vehicle is the least complex area to control the flow due to the fact that, with the side windows closed, there are no heated or rotating parts that interfere with the airflow such as for the wheel and wheelhouse section.

When studying the airflow past the greenhouse, it is shown that the windshield and A-pillar design controls how the flow along the greenhouse is developing and behaving. As for the front-end design, the windshield is the first contact in the interaction between airflow and the vehicle upper-body. A significant drag reduction can hence be obtained with an optimized windshield design.

Increasing the slope of the windshield tends to reduce the pressure at the base of the screen resulting in a lower contribution of drag. Another gain with a more sloped windshield is that the attached airflow along the vehicle bonnet is better maintained in the cowl area between bonnet, windshield and roofing. This results in reduced separations which keeps the the airflow smooth. (Barnard, 2009)

According to Hucho (Hucho, 1998), it is confirmed that the drag coefficient is reduced with the increase of windshield angle as shown in figure 3.5.

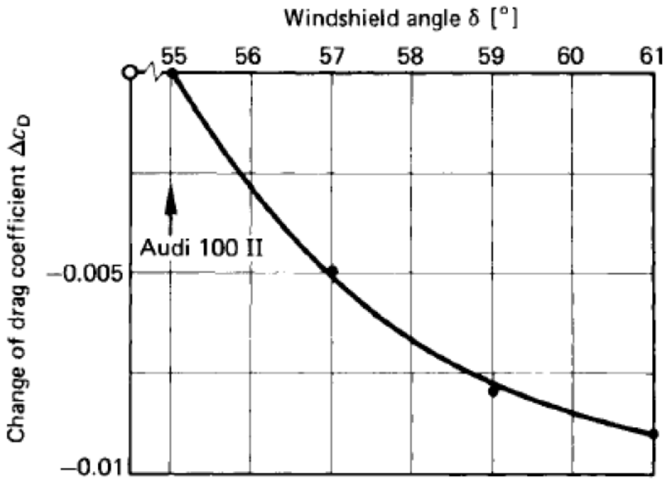


**Figure 3.5:** Windshield angle vs drag reduction (Hucho, 1998)

A largely sloped windshields are usually used in high-end sports cars in order to maximize the aerodynamic performance. However, today car manufacturers developing and producing passenger vehicles such as Tesla INC where aerodynamic performance is highly prioritized, an increased slope of the windshield, as shown in figure 3.6, is been implemented in the vehicles. The windshiled angle of the Model S is 66°. (Palin et al, 2012).


**Figure 3.6:** Tesla Model S, windshield slope angle

There is however a downsize with an increased windshield slope. Solar heating and internal reflection form the glass limits the angle of the windshield in a safety point-of-view.(Barnard, 2009)

Another large contribution to the aerodynamic drag from the upper-body is the loss of pressure in the wake region. With a roof slope angle, the pressure loss can be modified and hence improved. In their paper, R. Littlewood and M.Passmore (Littlewood, 2010), shows that increasing the roof slope angle to 12% gives the largest drag reduction as shown to the left in figure 3.7. With a further increase of the slope angle the drag coefficient starts rising. This behaviour is also seen in the study of R.F Soares and F.J De Souza (Soares et al, 2015) as shown to the right in figure 3.5. An angle of 10°-12° gives the largest drag reduction.

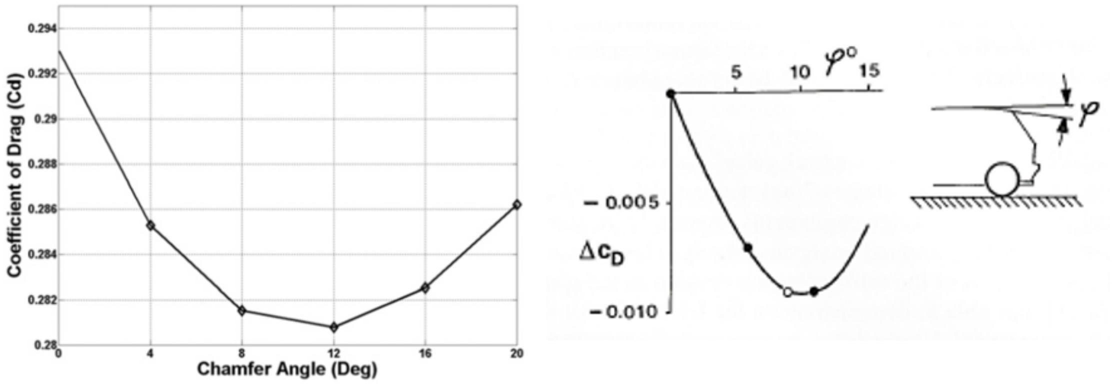


**Figure 3.7:** Roof slope angle vs drag coefficient

These large slope angles are widely used for sedan and fastback configurations. For SUV:s other requirements, such as the trunk volume limits the car manufacturer to increase the roof slope angle. Some exceptions, such as BMW X6, uses large roof slope angles which gives larger reduction is drag coefficient to the price of reducing the trunk volume. Different roof slopes are visualized in figure 3.8.


**Figure 3.8:** Roof slope angle for different SUV designs

In order to further control the airflow at the rear of the vehicle, spoilers are being used. Due to the fact that the rear upper-part differs for e.g. a SUV compared to a sedan, the spoilers look different although used for the same purpose. Rear spoilers are traditionally used to increase downforce at the rear-end of the vehicle, however new uses of the spoilers are developed and being implemented. With the new use of a roof and/or trunk spoiler, the airflow is further attached to the vehicle upper-body surface resulting in a delayed separation as shown in figure 3.9.

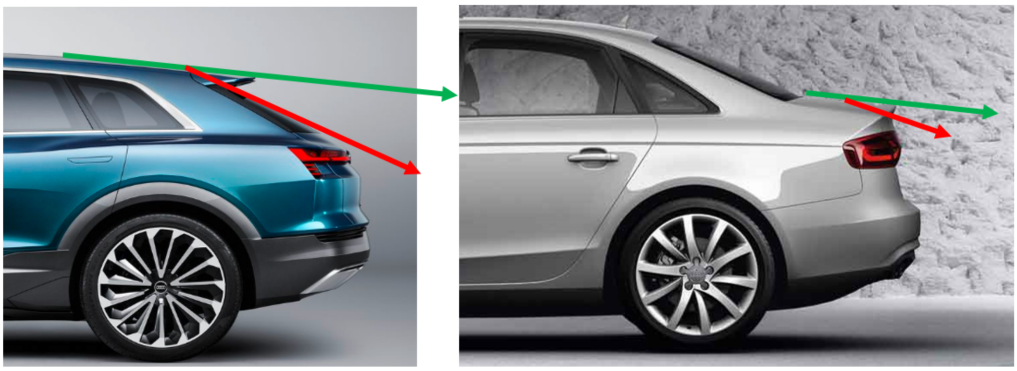

**Figure 3.9:** Flow path with(green)/without(red) roof and trunk spoiler

The delayed separation yields the recovery of the back pressure and hence reduces the wake size. This results in a reduction of drag according to Soares. (Soares et al., 2015) Other studies made by Ljungskog (Ljungskog et al., 2016) and Sebben (Sebben et al., 2014), shows that tuning the edges and angles of the spoilers allows for further drag reduction.

### 3.1.3 Rear-End

The rear-end of a vehicle is considered as the rear-end of a bluff body where the airflow along the vehicle separates and creates a low pressure area behind the vehicle. This results in a drag increase. In a study made by Hucho (Hucho, 1998), the influence of rear-end boat tailing on aerodynamic performance is investigated. Hucho found that, as shown in figure 3.10, by tapering the rear-end a drag reduction of 11-13% is possible. The study also showed that after a certain angle of the tapering, further reduction of the drag coefficient is not possible.

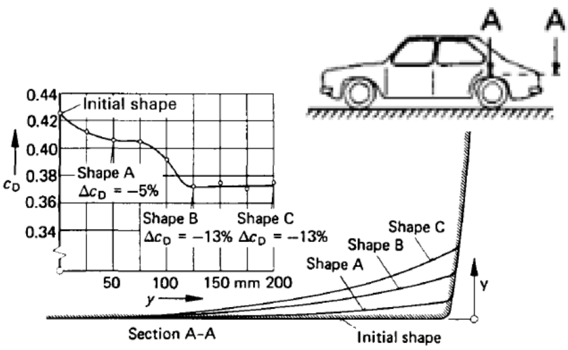


**Figure 3.10:** Hucho's studies and results for tapering the rear end. (Hucho, 1998)

Additionally to Hucho, Daryakenari (Daryakenari et al, 2013) made a similar study where the effect of tapering the rear-end on aerodynamic performance was investigated. Daryakenaris study was based on the Ahmed body and yielded the same results as Hucho's study hence a drag reduction of up to 11% as shown in figure 3.11.

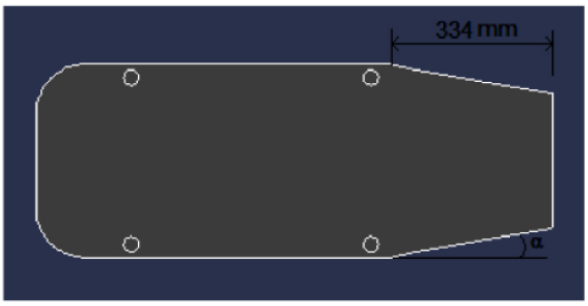


| α | ΔCd(%) |
|---|---|
| 1° | -5.44041 |
| 2° | -8.16062 |
| 3° | -9.58549 |
| 4° | -10.1036 |
| 5° | -10.8808 |
| 6° | -11.399 |

**Figure 3.11:** Daryakenari's studies and results for tapering the rear end. (Daryakenari et al, 2013)

In a study made by Kumar (Kumar et al, 2015), the aerodynamic development of the Suzuki Vitara Brezza was studied. Kumar discovered that using a sharp edge on rear-end sides resulted in a 2.2% reduction of the drag coefficient. This drag reduction is obtained by better flow attachment towards the rear-end and enhanced control of separation, especially for side winds. The use of a sharp rear-end side edge is started to be used in the current the vehicle models seen on the road. Figure 3.12 presents some examples of vehicles using a the sharp edge design.

**Figure 3.12:** Nissan Murano(left) and Tesla Model S(right) using a sharp rear-end edge.

In order to further delay the rear-end separation and hence allow for a large base pressure recovery, a paper published by Sterken (Sterken et al, 2014) describes the effect of using rear-end extensions on the aerodynamic performance. In this study, Sterken used a Volvo XC60 to base the investigations on and was able to obtain up to 5% reduction of the drag coefficient with the use of 250 mm extensions on the side and upper part of the rear-end, as shown in figure 3.13.

**Figure 3.13:** Sterken's experimental test setup for the rear-end extension (Sterken et al, 2014)

### 3.1.4 Under-Body

In a conventional vehicle, the underbody is the home of a large number of parts such as the exhaust pipes, mufflers, fueltank and in some vehicle configurations, a gearbox and a propulsion shaft. These parts are contributing to a large number of the total drag due the disruption of the airflow passing along the underbody of a vehicle. In order to reduce the airflow disturbance, studies have been made on the use of underbody panels. According to Sebben (Sebben, et al, 2016), the reduction of the drag coefficient with the use of different underbody panels and covers for a conventional passenger vehicle is shown in figure 3.14.

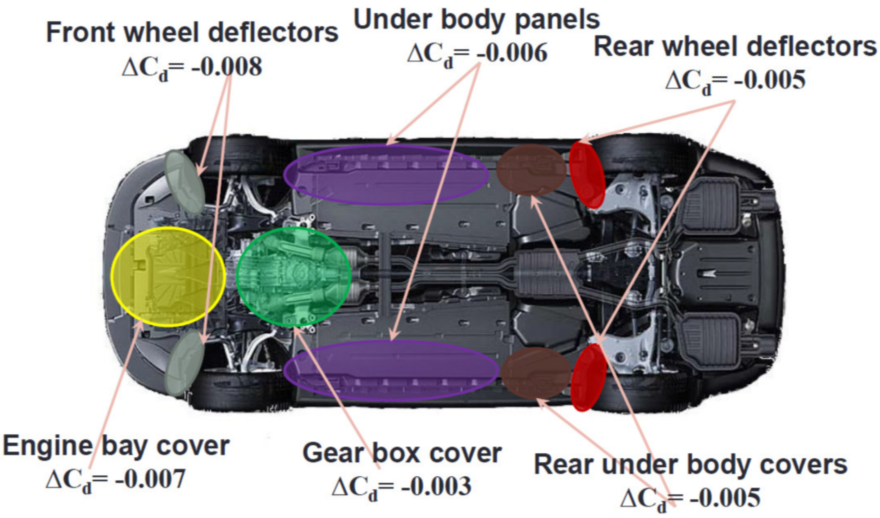


**Figure 3.14:** The effect of underbody panels on the Cd value (Sebben et al., 2016)

For electric vehicles, unlike conventional vehicles, a flat underbody is used due to the fact that the battery package is located between the wheelbase of the underbody. This placement of the battery not only improves the handling, stability and ride comfort due to the low center of gravity but also aids the aerodynamic performance.

Although a flat underbody contributes to a great aerodynamic performace of a vehicle, studies have been made in order to further improve it. A study made by Ishihara (Ishihara, 2011), shows that Nissan Leaf, which is a pure electric vehicle is using different types of underbody panels in order to further reduce drag by optimizing the underbody. In figure 3.15, the underbody panels used in Nissan Leag is shown. The panels include a large front undercover with an aero-optimized convex, a large flat floor cover with fins along the panel and a diffuser with large fins. These features are used to distribute and guide the air flow along the underbody in a highly efficient way in order to reduce drag.

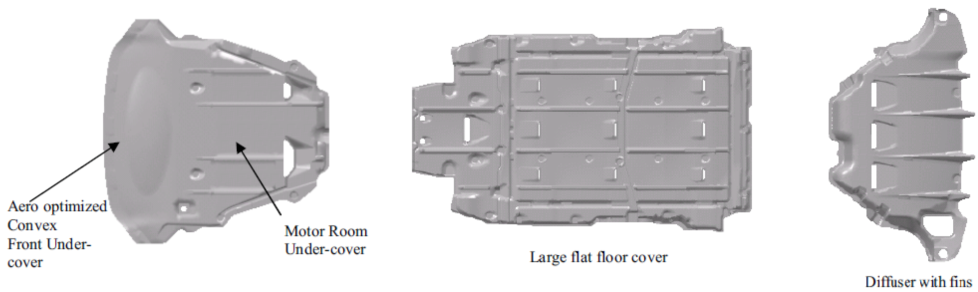


**Figure 3.15:** The underbody panels of Nissan Leaf.(Ishihara, 2011)

Other focus areas in order to enhance the aerodynamic performance of the underbody is the study of the diffuser. A diffuser is located at the end of the underbody and is used in order to reduce the airflow velocity exiting the underbody to increase the base pressure at the rear-end of the vehicle and hence reduce the wake size.

A study performed by Löfdahl (Löfdahl et al, 2013), investigates in the optimum diffuser angle for a sedan and a estateback configuration as shown in figure 3.16. In the study it is shown that a diffuser angle for a sedan results in significantly larger drag reductions than an estateback. An angle of 5°-8° resulted in the biggest drag reduction for both configurations.

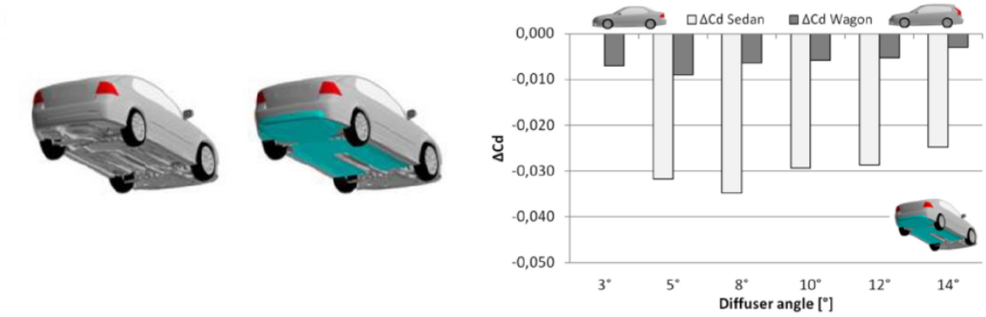


**Figure 3.16:** Diffuser study for a sedan and estateback vehicle configuration.

In order to further improve the aerodynamic performance of the diffuser, studies on diffuser extensions have been made such a study made by Kang (Kang et al, 2012). Kang shows that with a 400mm extended diffuser, a drag reduction of up to 6% can be obtained as shown in figure 3.17. Another interesting result is that the drag reduction differ with for different vehicle speeds.

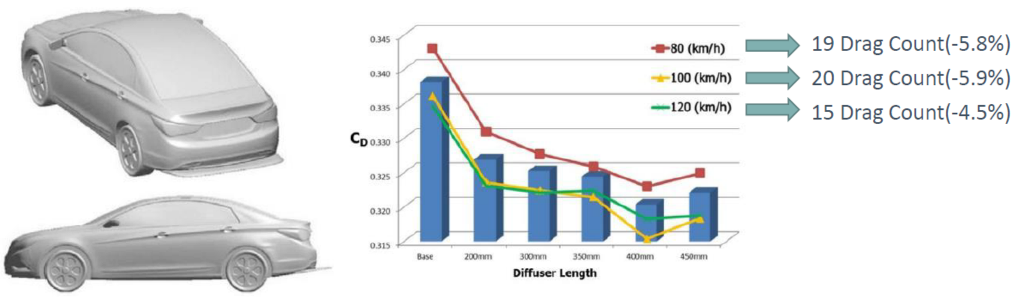


**Figure 3.17:** Study results of the length of diffuser extensions.

To further improve the result of the extended diffuser, Kang also studied the design of the extensions as shown in figure 3.18. It was found that the largest drag reduction is obtained with a arc plate shape of the extension.

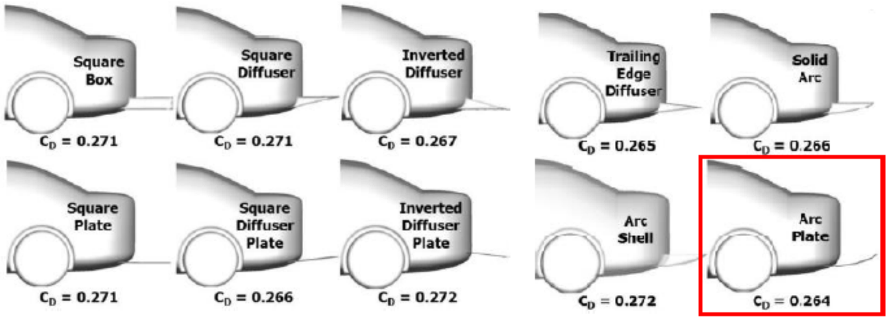


**Figure 3.18:** Diffuser extension designs vs Cd value.

### 3.1.5 Wheels

The wheel rims used in vehicles come in different sizes and designs. Some of the rim designs benefit the aerodynamic performance of vehicles and some works opposite the aerodynamics hence increasing drag. A study made by Vdovin (Vdovin, 2013) shows various rim designs and their impact on the aerodynamic resistance. In the study, Vdovin found that a rim design with a thick outer radius followed by a fully closed rim design, as shown in figure 3.19, gave the best aerodynamic results.

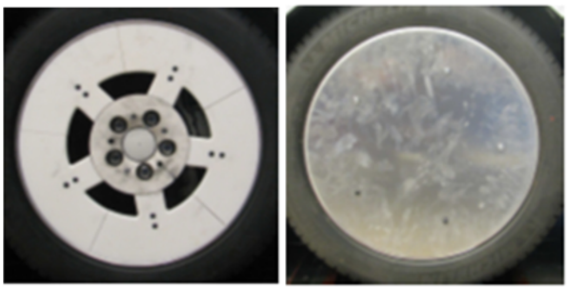

**Figure 3.19:** Best aerodynamic rim designs according to Vdovin

The main issue with the fully closed rim is that it prevents the airflow to access and cool the brakes through the rim. Renault Ecolab (Renault, 2017) have come up with a solution for this by using an active rim design as shown in figure 3.20.

**Figure 3.20:** Aerodynamimc rim design used in Renault Eolab

During a highway drive with a constant velocity and where the brakes are barely engaged, the rims goes into a fully closed state to reduce the aerodynamic energy loss that a open rim causes. In a driving situation such as driving downhill with a constant velocity the brakes are constantly engaged making the rims go into a fully open state to let the air flow pass through the brakes to act as a cooling fluid. Other types of aerodynamically designed rims are rims with fanblade shapes. These type of rims are used by Tesla in all their vehicles. A more detailed description can be found in (Palin et al, 2012) where this is studied.

## 3.2 Regulations regarding the Rear View Side Mirrors

Rear view side mirrors (RVSM) are today mandatory in automobiles to increase the safety (Esser, 2016). The RVSM gives the driver a side view when changing lanes and a rear view to aid reversing. Another way of visualising the surroundings of a vehicle is by using a Camera Monitoring System (CMS). As the cameras are getting smaller in size and cheaper, car manufacturers are starting to use them to e.g. giving a 360°-view around the car. The CMS is allowed to be used to aid visibility but is not permitted to replace the RVSM.

A first step on the way to replace the mandatory RVSM with a CMS is the UN Regulation No. 46, which came into force 2013 (Esser, 2016). Today the regulation is adopted by a large number of countries, however not by China and the US. In his paper, M. Esser shows that it is up to every country to decide whether or not to apply it on a national level. It is also told that authorities within a country are demanding evidence that the CMS technology provides the same or better safety level than the RVSM in order to approve it. The leading country in which the CMS can replace the RVSM in the near future is Japan.

In an aerodynamic aspect, RVSM correspond to 6% of the total drag coefficient of a vehicle whereas a CMS system could reduce it to 2% of $Cd_{tot}$ (Esser, 2016). In figure 3.21, the difference in RVSM versus CMS size is shown.

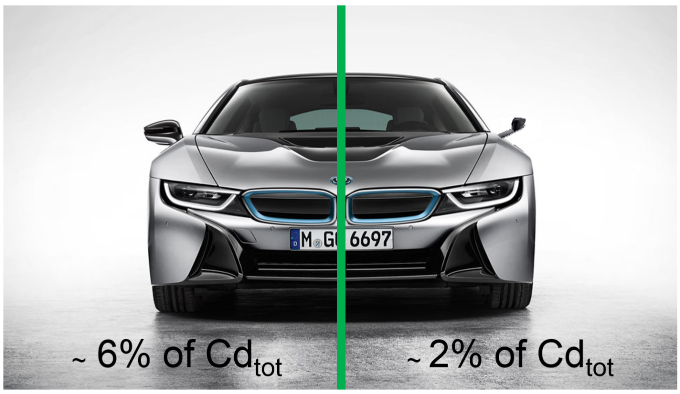


**Figure 3.21:** RVSM vs CMS size and its impact on the total drag coefficient

# 4
# Plan of Concepts

Finalizing the benchmarking study and the literature review, a large number of features and design recommendations which benefits the aerodynamic performance of a vehicle are found. A concept screening is then necessary in order to make the investigation realistic considering the aspects of time and resources such as cluster queuing and usage. All findings are however worth investigating in due to their drag reducing characteristics.

Together with the CFD team at NEVS, a couple of concepts were chosen for further investigation. These concepts were chosen in a way that would give the largest benefit for NEVS and aid their work in improving the aerodynamics of their vehicles. At the same time, the chosen concepts are based on the benchmarking study and the aerodynamic features found. The main focus of this study is to the develop aerodynamic features which can be implemented in the near future.

In figure 4.1, the different concepts are presented. The figure also presents the different phases in which the concepts are divided into.

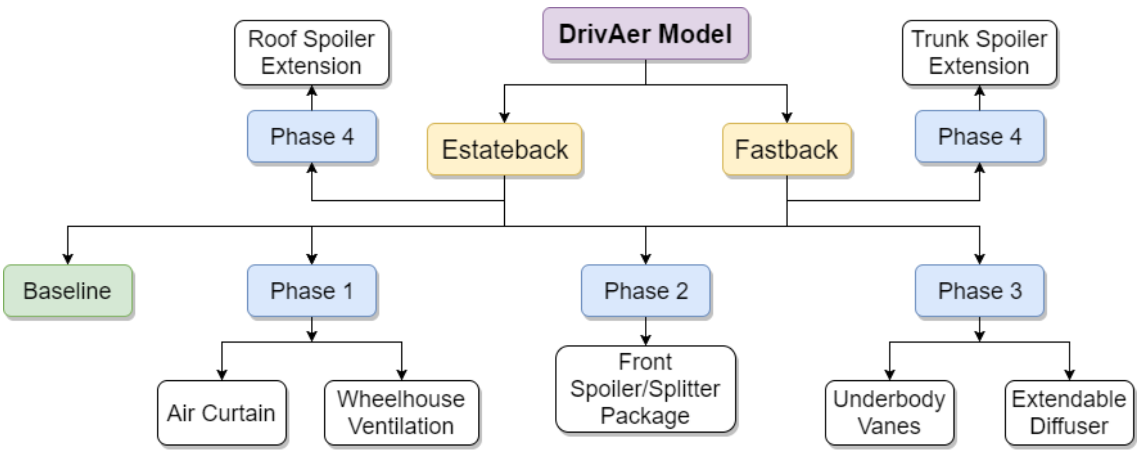


**Figure 4.1:** Case setup describing the concepts that are to be investigated.

The first phase focuses on the front-end and the front wheelhouses of the vehicle. Since the electric vehicle does not need a big cooling package, the front end of the vehicle can be modified and improved with aerodynamic features. Today the usage of air curtains are becoming popular for passenger vehicles. The idea with an air curtain is that by the use of a narrow channel at the front bumper corners, speeding up the airflow to guide it past the front tire. Due to the fact that there is poor literature published that studies this feature, the air curtain was chosen for investigation. Additional to the air curtain feature, a wheelhouse ventilation was chosen to be studied in the first phase. The wheelhouse ventilation is widely used in sports cars and luxury vehicles and nowadays this feature is started to be implemented in passenger vehicles in order to improve the aerodynamic performance. As for the air curtain, poor literature is published which made it interesting to study the impact of an wheelhouse ventilation.

In the second phase, the front spoiler/splitter package was chosen to be studied. The idea to investigate in the effect of a front spoiler/splitter package is that even though electric vehicles has a smooth underbody causing no disturbance in the airflow, the effect of a further reduction of the airflow under the vehicle seemed interesting. This due to Robinette's study which showed that the drag reduction might reach up to 20%.

In the third phase of this study, the focus was on the underbody. A Nissan Leaf paper (Ishihara et al., 2011) where the aerodynamic development of the vehicle was studied showed that even though the car have a flat underbody, the airflow along it can be improved with the use of underbody vanes. As NEVS is developing electric vehicles where flat underbodies might be used, studying the influence of underbody vanes was chosen for further investigation.

Additional to the underbody vanes, another concept for the underbody study is the diffuser extension which from the benchmarking is found to be an active aerodynamic feature. The diffuser extension is today used in concept vehicles and will most likely be implemented in production vehicles in the near future. Literatures on the diffuser extension shows that a drag reduction of up to 6% is possible for a conventional vehicle without the use of a flat underbody. The fact that the diffuser extensions impacts on the wake of the vehicle and no studies have yet been made for an electric vehicle, it was chosen for further investigation.

In the fourth and last phase, just like for the diffuser extension another active aerodynamic feature was chosen to be studied. In this case the rear upper-body of the estateback and fastback configurations were investigated using a roof spoiler extension for the estateback and a trunk spoiler extension for the fastback. These features are as for the diffuser extension only used in concept vehicles but are likely to be implemented in production vehicles in the near future. As these features also affects the wake size by delaying airflow separation and possibly improving the aerodynamic performance, they are chosen for investigation.

All concepts in phase 1-3 are identical for both the estateback and fastback configuration. The concepts are designed to enhance the aerodynamic performance of the DrivAer model. This is done by postprocessing the baseline simulation and deciding on where to place and how to design the different concepts. In chapter 8, a detailed description of the concept design together with the baseline results are presented.

# 5

# DrivAer Model

The DrivAer model is a vehicle model developed in a joint project between BMW, Audi and the institute of aerodynamics and fluid mechanics of the Technical University of Munich. This project was conducted in order to develop a generic vehicle model intended for aerodynamic studies. The DrivAer model is used both in the automotive industry and in the academic world to reduce the simulation gap between simplified models, such as the Ahmed body (Barnard, 2009) and more complex "actual car" geometries (Heft et al, 2012).

Today, many aerodynamic studies are still based on the Ahmed body. The Ahmed body is however a very simple model and do not represent the geometry of an "actual car", making the simulation results not accurate enough to be transferred to an "actual car" geometry.

Another advantage using the DrivAer model is that it is available in different configurations, as shown in figure 5.1. This increases the accuracy and reduces the simulation gap between e.g an fastback configuration of the DrivAer model and a similar configuration in another vehicle model.

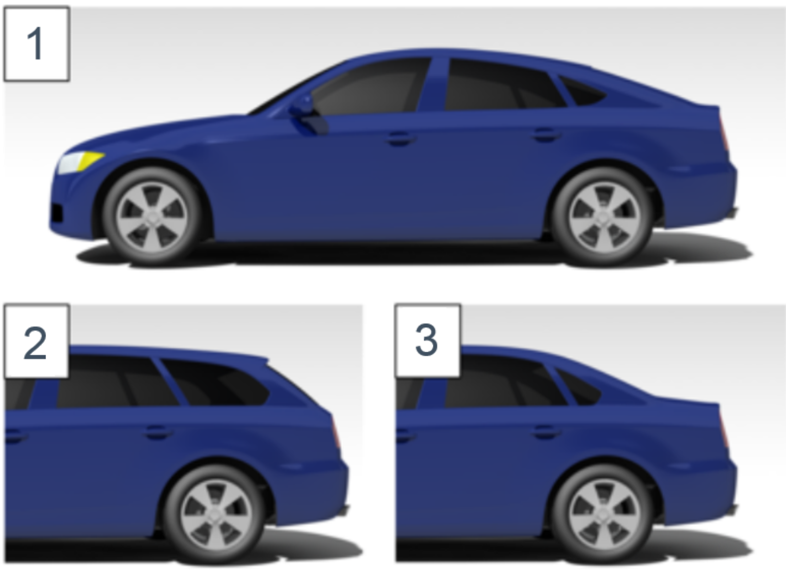


**Figure 5.1:** Different configurations of the DrivAer model: 1-Fastback, 2-Estateback, 3-Sedan

In this thesis, the fastback and the estateback configurations are chosen to investigate the chosen concepts on. This decision is made together with NEVS in which the company's interest is highly valued.

The DrivAer model comes with a detailed engine bay where an conventional engine, an exhaust system, a gearbox and a heat exchanger package with two grille openings are included. Due to NEVS being a developer and producer of electric vehicles, the engine and gearbox is replaced by geometries corresponding to a generic electric motor, an inverter and a new front wheel drive gearbox. In the heat exchanger package, the upper grille opening is closed. This modification was done with the help of NEVS and the final configuration is shown in figure 5.2.

Other configurations which are used is a completely smooth underbody panel and open rims.

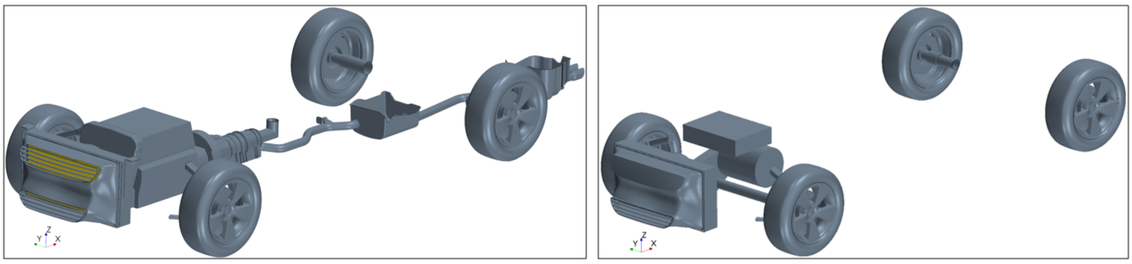

**Figure 5.2:** Engine bay modification of the DrivAer model: conventional drivetrain (left), electrical drivetrain (right)

As the DrivAer model still have a cooling opening in the lower part of the front-end after modifying the vehicle to correspond to an electric vehicle, outlets for the cooling flow entering through the lower front grille were created. These outlets are placed in the front wheelhouses as seen in figure 5.3.

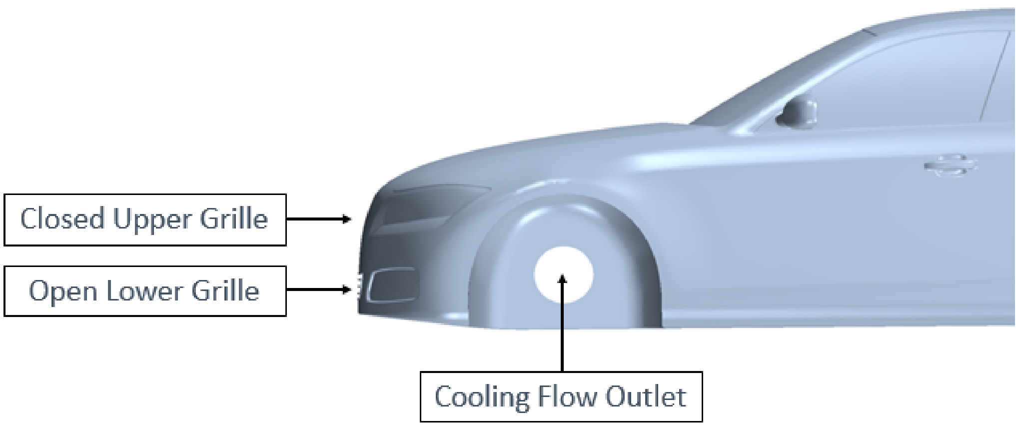


**Figure 5.3:** Inlets and outlets for the DrivAer model engine-bay cooling flow

# 6 Theory

## 6.1 Fluid Dynamics

A fluid is characterized by its different states. These corresponds to a laminar, a turbulent and a laminar-turbulent transition state. Further the different fluid states are defined by a Reynold's number, Re as presented in expression 6.1 where U is the fluid velocity , L is the length of the interaction between the fluid flow and the geometry and $\mu$ is the viscosity of the flow.

$$Re = \frac{UL}{\mu} \tag{6.1}$$

The Re number is dimensionsless where Re <= 500 000 corresponds to a laminar flow and Re > 500 000 corresponds to a turbulent flow. Comparing the different states, a laminar state is characterized by a smooth flow which is easy to predict due to the streams following the flow velocity. The turbulent state, however, is characterized by an irregular three-dimensional flow behaviour and is thus hard to predict. (Anderson et al., 2016)

A vehicle driving in a highway have a highly turbulent and three-dimensional air flow exerted to it. Before hitting the front end of the vehicle, the flow is laminar hence following the ambient wind velocity. After hitting the vehicle front end, the laminar state of the fluid is transformed along the vehicle surface to a turbulent state at the rear-end of the vehicle due to vehicle design and disturbances in the flow path. A wake is created behind the vehicle as a result of the described flow behaviour.

In this thesis, the vehicle is simulated in a highway drive with a velocity of 120 kph which results in a Re number more than 9 500 000.

### 6.1.1 Compressibility

In order to decide on which computation model to use for the CFD setup, the compressibility of the fluid flow must be determined. This is done by using the Mach number, Ma which relates to the compressibility of a fluid flow. In expression 6.2, it is shown how the Ma is calculated where U is the flow velocity and $v_s$ is the speed of sound.

$$Ma = \frac{U}{v_s} \tag{6.2}$$

According to Andersson (Anderson et al., 2016), a fluid flow with a Ma number less than 0.3 is considered as an incompressible flow. As the vehicle is driving in 120 kph in this thesis, the Ma number is calculated to be 0.098 making the flow incompressible.

## 6.2 Turbulence Model

Due to the flow being incompressible, the main and most used turbulence model to simulate and evaluate the behaviour of the flow are the Reynold's Averaged Navier-Stokes equations, RANS model (Andersson et al., 2016). In expression 6.3, the governing equation for RANS is shown.

$$\rho(\underbrace{\frac{\partial \mathbf{v}}{\partial t}}_{\substack{\text{Unsteady}\\ \text{acceleration}}} + \underbrace{\mathbf{v}\nabla\mathbf{v}}_{\substack{\text{Convective}\\ \text{acceleration}}}) = \underbrace{-\nabla p}_{\substack{\text{Pressure}\\ \text{gradient}}} + \underbrace{\mu\nabla^2\mathbf{v}}_{\text{Viscosity}} + \underbrace{\mathbf{f}}_{\substack{\text{Other}\\ \text{body}\\ \text{forces.}}} \tag{6.3}$$

In a fluid flow, turbulent and non-turbulent states are mixed together. To simplify the calculations and reducing computational time, the RANS equations separates these two fluid states and uses a statistical method to compute the velocity and the turbulent behaviour of a fluid flow. (Andersson et al., 2016)

In order to complete the turbulence model and hence improve the accuracy, a two-equation transport equation is used.

### 6.2.1 Two-equation Transport Model

Considering the computational resources available and NEVS standards, the k-$\omega$ was chosen as a two-equation model due to its performance in regions with adverse pressure gradients and separating flows (Andersson et al., 2016). For external aerodynamics such regions corresponds to the complex boundary layer between flow and surface.

To be able to resolve the kinetic energy, k and the turbulent frequency, $\omega$ as the k-$\omega$ model does, it needs a very fine mesh close to the surface of the geometry. A wall $y^+$ value of less than 5 is required. (Andersson et al., 2016) The $y^+$ value defines the inner stresses of a near-wall region where a no-slip condition (Andersson et al., 2016) is present. The inner stresses correspond to shear stresses which are developed due to the viscosity of the fluid when interacting with a surface.

An addition to the k-$\omega$ model is the Shear Stress Transport equation, SST which uses the k-omega in the near-wall region but also uses the k-$\epsilon$ model in the free flow stream. This results in an increase of the computational accuracy of the flow separation under an adverse pressure gradient. (Andersson et al, 2016)

### 6.2.2 Energy Model

The energy modelling in StarCCM+ is done by choosing between two approaches, either by using a coupled flow model or a segregated flow model. For an incompressible flow, the segregated flow model is the most used approach and is used in this thesis. (Pascau et al, 1996) Another advantage with the segregated flow model is that it solves the energy equations sequentially and hence does not require large computational resources.

## 6.3 Porous Medium

In the heat exchanger package of the DrivAer model, a radiator is included. Do to the tiny channels of the radiator, the mass flow of the air flow through the channels is slowed down, hence creating a pressure drop between the inlet and outlet of the radiator. To simulate this pressure drop in a CFD environment, a porous medium is created using Darcy's Law as shown in expression 6.4

$$-\frac{\Delta p}{\Delta x} = \underbrace{\frac{150\mu(1-X)^2}{X^3 D_p^2}}_{\text{Viscous porous resistance}} v + \underbrace{\frac{1.75\rho(1-X)}{X^3 D_p}}_{\text{Inertial porous resistance}} v^2 \tag{6.4}$$

where Δp corresponds to the pressure drop and Δx to the radiator width. In StarCCM+, both the viscous porous resistance and the inertial porous resistance expressions are inserted as constants. In appendix A, a detailed calculation of these constants are shown where the data used to calculate these constants corresponds to a generic radiator pressure drop.

## 6.4 Air Resistance Forces

A vehicle driven in any velocities are exerted to counteracting forces in form of air resistance. This resistance force is created by the sum of friction and pressure on the geometry. The more streamlined a geometry is the less air resistance is produced. The increase and decrease of air resistance is known as an aerodynamic performance.

To be able to compare the aerodynamic performance between different geometries, e.g. Vehicle shapes, a dimensionless parameter is used. This parameter is called drag/lift coefficient, Cd/Cl and is calculated using the forces exerted on the geometry as shown in equation 6.5.

$$F_{drag/lift} = \frac{1}{2}\rho C_{D/l} A_f v^2 \tag{6.5}$$

Vehicle velocity and density are most often constant values due to standardized test methods however the frontal area differs between geometries. The Cd/Cl values are often very low in magnitude and to make it easier to display and to discuss these parameter it is usually mentioned as counts, where 1 count correspond to 0.001Cd/Cl.

# 7
# Methods

## 7.1 CAD Preparation and Cleanup

To make the DrivAer model ready for simulation it needs to be cleaned. Cleaning the model means that intersecting, overlapping faces and surfaces are redesigned and corrected. This makes the model topographically correct which facilitates meshing and the simulation setup. Additionally the mesh quality is further improved.

The CAD cleaning is performed in ANSA (ANSA, 2017) and the geometry is checked for proximities, intersections and unwanted gaps. When this is done, a surface mesh is created in order to export the geometry in a stl format which only contains the elements of the mesh and not the surface of the geometry. This file format is widely used and can be imported in any CAE/CFD softwares.

To enhance the meshing created in the CFD software, StarCCM+ (StarCCM+, 2017), and to capture the simulation results by e.g looking at forces exerted on different parts or following the air flow along specific areas, the car geometry is divided into different part ID:s.

## 7.2 Windtunnel Setup

In order to capture the flow behaviour around the vehicle during a highway drive, a windtunnel is created in the CFD environment. The dimension of the windtunnel and the placement of the vehicle model is set according to the StarCCM+ (StarCCM+, 2017) documentation and is shown in figure 7.1.

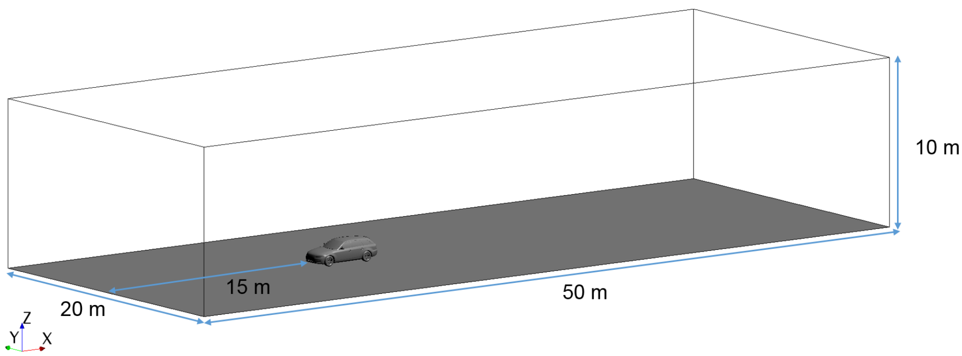


**Figure 7.1:** Windtunnel dimensions according to StarCCM+ recommendations

These dimensions are taken the influence of the domain boundaries into account by making the windtunnel large enough. This is one big advantage with using CFD compared to a windunnel. In a windtunnel test it is difficult to get rid of the influence of the domain boundaries due to fan capacity and available space.

## 7.3 Mesh Generation

A mesh generation includes a surface mesh in order to capture the flow phenomena which interacts with the surface of a geometry and a volume mesh in order to capture the flow in the domain.

### 7.3.1 Surface Mesh

A surface mesh is created using a surface wrapper and a surface remesher. The surface wrapper is used in order to close gaps in the vehicle geometry where an airflow is not desired. This procedure makes the vehicle geometry "waterproof". A surface wrapper alone does not give a good enough mesh quality but can be improved by the use of a surface remesher. The surface remesher improves the mesh quality by re-triangulating the surface mesh created by the surface wrapper.

Both the surface wrapper and the surface remesher are used and controlled by the surface mesh option in StarCCM+. The surface mesh is created by defining a base cell size for the whole vehicle geometry. In order to improve the mesh in areas with complex geometries or parts with dimensions smaller than the base cell size, surface controls can be used. As the vehicle geometry was divided into different PID:s in ANSA, custom cell sizes was given to different PID:s in order to enhance the mesh quality.

The base cell size is set to 20mm and reaches a minimum of 2mm in the most complex areas of the vehicle geometry.

### 7.3.2 Volume Mesh

The volume mesh is created with the trimmer method, recommended by the Star-CCM+ documentation. The Trimmer method uses hexahedral cells and allows for refinement boxes to increase the accuracy of the simulation in areas with highly complex flow behaviour.

In this thesis, an accurate Cd value is not very important due to the fact that the difference of drag coefficients and trends between concepts are more prioritized. Two baseline simulations were performed, one with a volume mesh of 25 million cells and one with a volume mesh of 45 million cells. Taken the computational time into account, the results given by the 25 million cells case compared to the 45 million case is considered good enough. A decision was made to run all simulations with a volume mesh consisting of 25 million cells.

#### 7.3.2.1 Refinement Boxes

Refinement boxes are used in order to capture the flow behaviour in areas where the flow is the most complex. These areas include the flow near the vehicle, the wake of the vehicle and the area between the underbody and ground surface, as shown in figure 7.2.

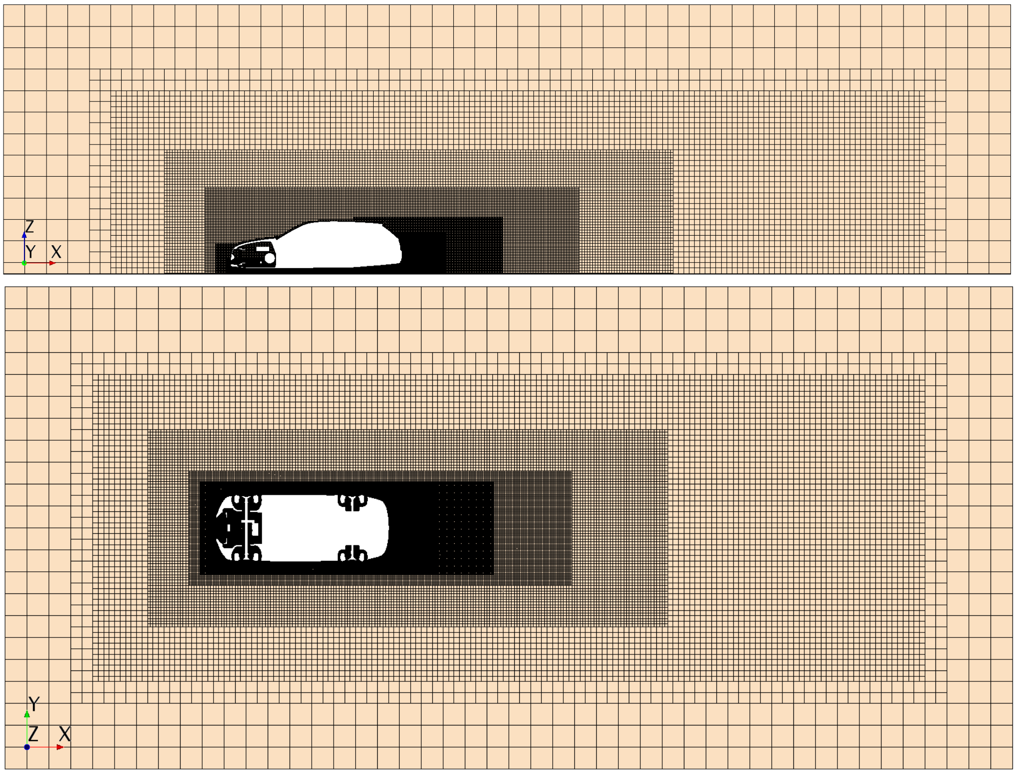


**Figure 7.2:** Refinement boxes in order to accurately capture the flow behaviour.

Seven refinement boxes are used with different cell sizes in order to avoid a sudden increase between the zones. The finer box has a cell size of 14mm which is progressively increasing to meet the maximum cell size of the windtunnel, which is set to 720mm.

#### 7.3.2.2 Prism Layers and y+ values

At the vehicle surface, so called the near-wall boundary, a significant amount of drag is produced by the air friction. To capture the flow-to-surface interference, the y+ values are used and are set and controlled by creating prism layers.

As described in the theory chapter, with the use of the k-omega turbulence model, a y+-value between 0-5 is required to resolve the boundary layer. The first prism layer is set to 0.05mm followed by a total prism layer thickness of 3.5mm as shown in figure 7.3. A growth rate of 1.3 is set in order to, as for the refinement boxes, avoid a sudden increase between the prisms and the volumetric cell size.

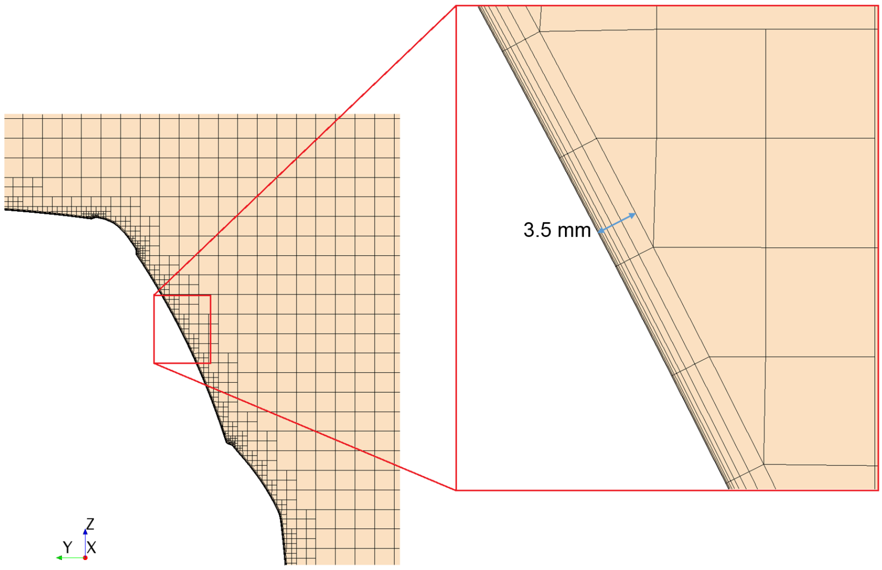


**Figure 7.3:** Prism layers at the vehicle surface

In figure 7.4, the resulting wall $y^+$ values for both the estateback and fastback configuration are shown. As seen in the figure, most of the values are between 2-3, however in the mirror and some of the front tire edges the wall $y^+$ value reaches the limit of 5. This is considered good enough considering the available computational resources.

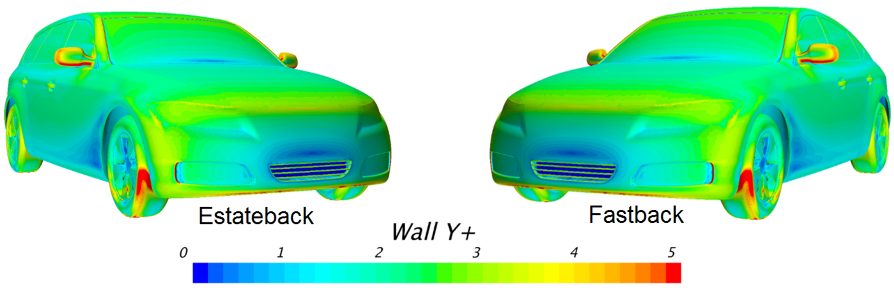


**Figure 7.4:** Wall y+ values at the vehicle surface for both configurations

## 7.4 Boundary and Physics Setup

The simulations are representing a vehicle moving in a straight forward direction with a velocity of 120 kph. The ground boundary is given a tangential velocity of 120 kph in x-direction to represent a moving vehicle. To get the wheels, brake disks and driveshafts to correspond to the simulated case a rotational speed is given, $\omega$ which is calculated as shown in expression 7.1.

$$\omega = \frac{v}{r} = \frac{120/3.6}{0.318} = 104.8[rad/s] \tag{7.1}$$

where v is the velocity and the r is the wheel radius.

For the boundaries of the windtunnel, the inlet is set to a velocity inlet boundary with the same velocity and direction as for the ground. The outlet is set to a pressure outlet boundary with a physics value of 0 to ensure that the outlet pressure keeps the same magnitude as in the domain. Both side walls and the sky are given a symmetrical boundary and the ambient temperature in the windtunnel is set to 25°C. In table 7.1, a sum up of the boundaries, conditions and physics values are presented.

**Table 7.1:** Boundary setup with conditions and physics values

| **Boundary** | **Condition** | **Physics value** |
|---|---|---|
| Ground | Tangential Velocity, v [kph] | [140, 0, 0] |
| Inlet | Velocity Inlet, v [kph] | [140, 0, 0] |
| Outlet | Pressure Outlet, P [Pa] | 0 (101325) |
| Wall/Sky | Symmetry | - |
| Front/Rear Wheels/Shafts | Rotational Velocity, $\omega$ [rad/s] | 104.8 |

As the k-$\omega$ model is used to compute the fluid dynamics and capturing the flow behaviour when interfering with the vehicle in the domain, additional in-model tools are available to increase accuracy. In table 7.2 the used tools are presented.

**Table 7.2:** Physics Setup

| **Physics Setup** |
|---|
| All $y^+$ Wall Treatment |
| Cell Quality Remediation |
| Constant Density |
| Exact Wall Distance |
| Gas (Air) |
| Gradients |
| K-Omega Turbulence |
| Reynolds-Averaged Navier-Stokes |
| Segregated Flow |
| SST (Menter) K-Omega |
| Steady |
| Three Dimensional |
| Turbulent |

# 8

# Baseline Run and Concept Design

In this chapter, the design parameters of the concepts are shown and explained. The concept designs are based on the baseline result for both the estateback and fastback configuration. As the geometry of both vehicle configurations is similair except the rear upper-body, most of the concept designs are created and simulated with the same parameters. The only difference in the concept design for both configurations is in the phase 4 where for the estateback configuration, a roof spoiler extension is investigated while for the fastback configuration a trunk spoiler extension is investigated.

## 8.1 Air Curtain

The purpose of an air curtain is that the narrowing channel at the corner of the front-end speed up the air stream and guide it past the front wheelhouse. As a result, this feature allows for the reduction of the interaction between the outer airflow and the front part of the tire resulting in reduction of drag. Since there are poor literature published about the air curtain, the air curtain used in this study is created by benchmarking the use of air curtains in today's vehicles and by analyzing the result of the baseline model simulation. Figure 8.1 shows the pressure coefficient at the front-end surface of the vehicle. The marked areas highlights the low pressure sections which corresponds to a high velocity airflow. The concept idea is to use the high velocity airflow by creating an inlet channel with an outlet in the wheelhouse.

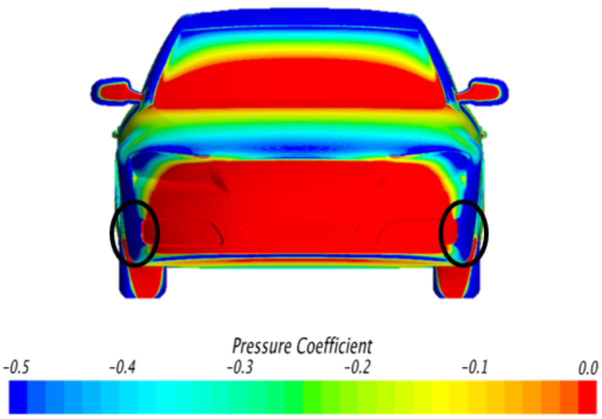


**Figure 8.1:** Pressure coefficient on the front-end of the baseline model.

After deciding on the placement of the air curtain inlet and outlet, the dimensions of the concept and its alternatives are decided. The inlet of the air curtain has a width of 20mm and a height of 150mm for all concepts. For the outlet, the same height as the inlet is used, however three different widths are created. These are 10mm, 20mm and 30mm. The air curtain design is shown in figure 8.2.

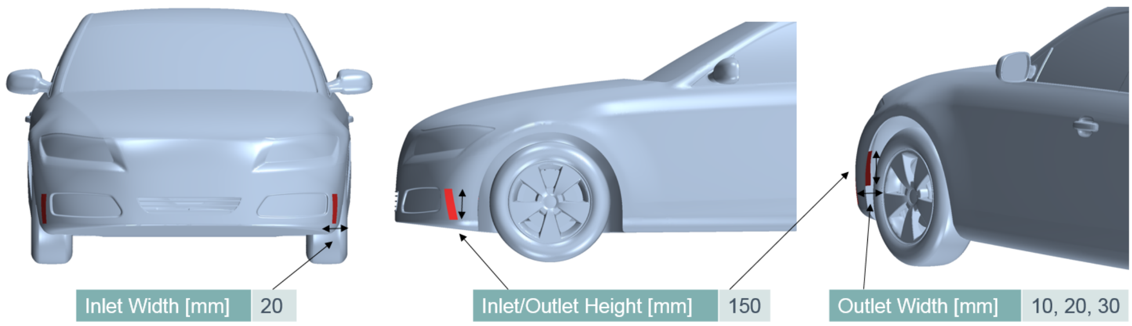


**Figure 8.2:** Design parameters of the air curtain concept.

## 8.2 Wheelhouse Ventilation

The purpose of a wheelhouse ventilation is to create an additional exiting path for the flow in the wheelhouse. Due to the fact that poor literatures were found about the wheelhouse ventilation, the concept design is based on benchmarking and the baseline result. In figure 8.3, the pressure coefficient distribution of the rear part of the wheelhouse is presented.

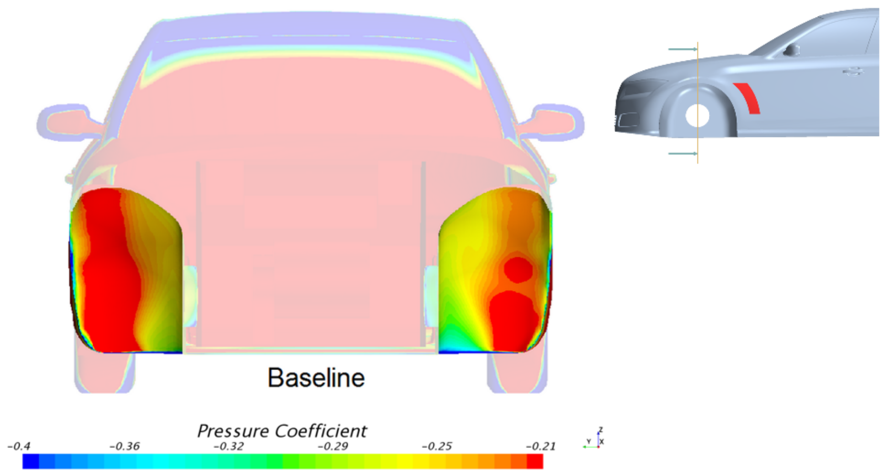


**Figure 8.3:** Pressure coefficient of the wheelhouse of the baseline model.

As seen, large stagnation areas are created by the airflow entering the wheelhouse resulting in high drag contribution. In order to reduce these stagnation areas, a wheelhouse ventilation is created near the wheelhouse arc with an inlet with of

50mm. The outlet width is kept the same as the inlet and the only changing parameter for the different cases is the height of the ventilation. Four different heights: 100mm, 200mm, 300mm and 400mm are decided to be investigated. In figure 8.4, the design of the wheelhouse ventilation is shown.

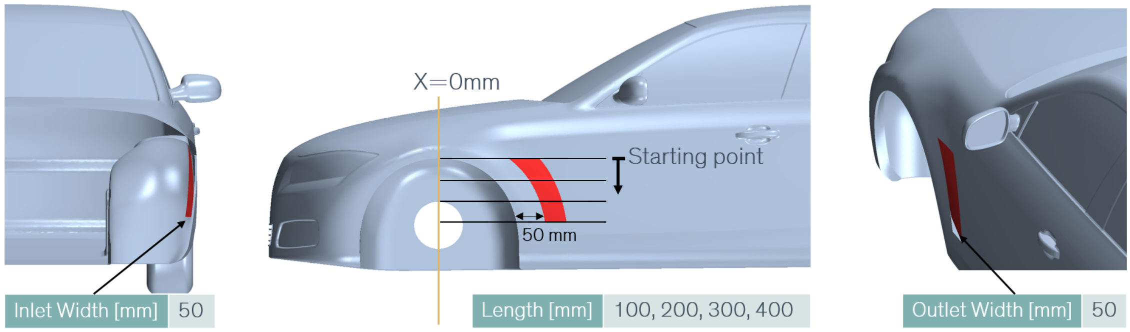


**Figure 8.4:** Design parameters of the wheelhouse ventilation concept.

## 8.3 Front Spoiler/Splitter Package

The front spoiler/splitter package is mainly used to reduce the airflow along the underbody of a conventional vehicle. In order to study the influence of a spoiler/splitter package in a electric vehicle, Robinette's study was used as an inspiration. The splitter width is set to 50mm and is kept the same for all cases and the only changing parameter is the spoiler height which is set to 40mm, 80mm and 120mm. In figure 8.5, the design of the spoiler/splitter package is shown.

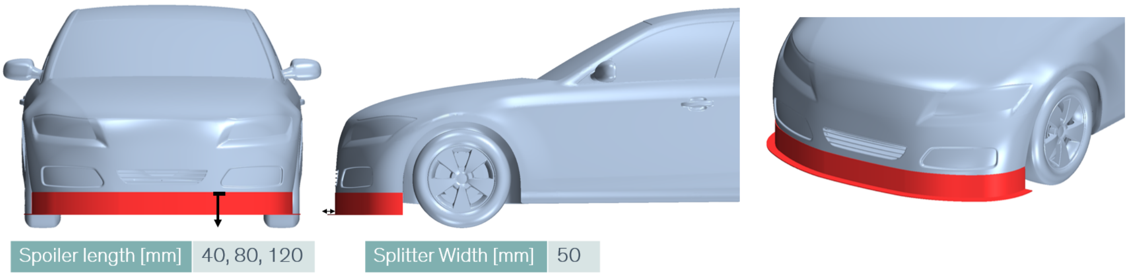


**Figure 8.5:** Design parameters of the front spoiler/splitter package concept.

With the 80mm and 120mm case of the concept, the frontal area of the vehicle is increased for both the estateback and fastback configuration.

## 8.4 Underbody Vanes

The guiding vanes are created in order to improve the distribution of the underbody flow. As seen in figure 8.6, the streamlines describing the underbody flow of the baseline runs for both the estateback and fastback configuration have the same behaviour. At the rear part of the underbody, as highlighted in the figure, the flow is directed towards the right side of the vehicle.

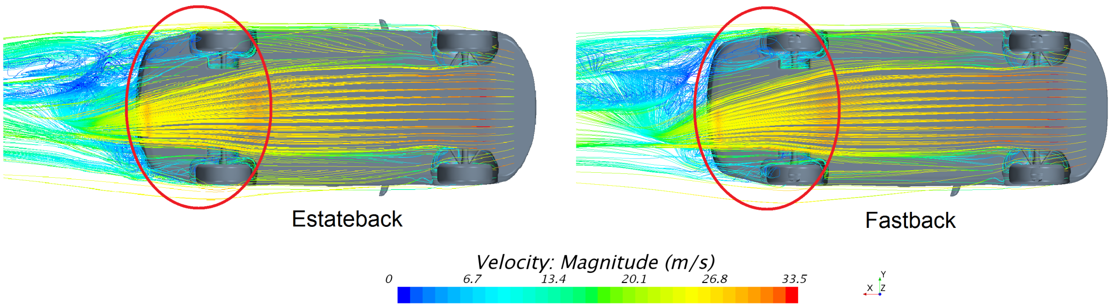


**Figure 8.6:** Underbody flow behaviour of the baseline models.

This behaviour is caused by a difference in the massflow of the air exiting the engine-bay outlets, located in each front wheelhouse. In figure 8.7, the iso surface of the wake for both configurations are shown. It is clearly seen that the flow on right and left side is not symmetric.

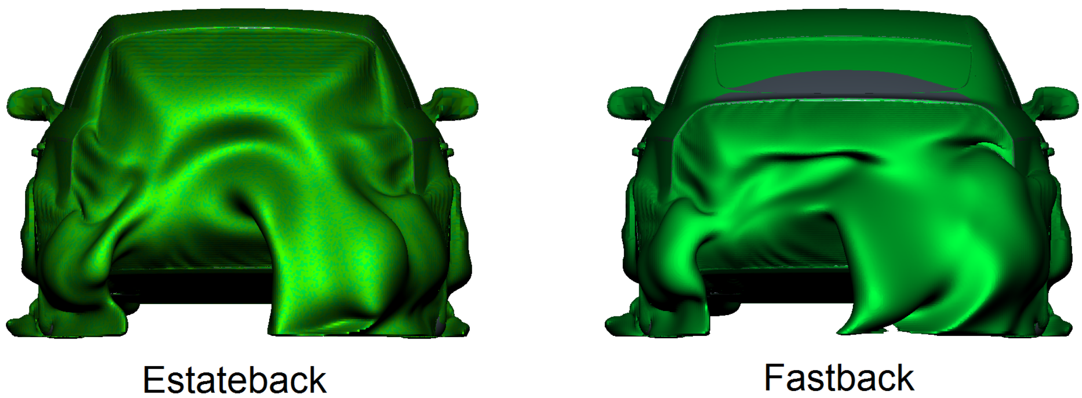


**Figure 8.7:** Isosurface of the wake for the baseline models.

Due to the different massflows, the pressure distribution between the right and left side of the vehicle is not the same as seen in figure 8.8. A higher overall pressure is obtained on the left side compared to the right side, resulting in a suction effect where the flow goes from a high pressure area to a low pressure one. The underbody flow tends to direct itself to one side starting at the end of the front wheelhouses. Due to the fact that the airflow is not interacting with the rear-end separation, a significant flow deviation to the right of the vehicle is not noticable.

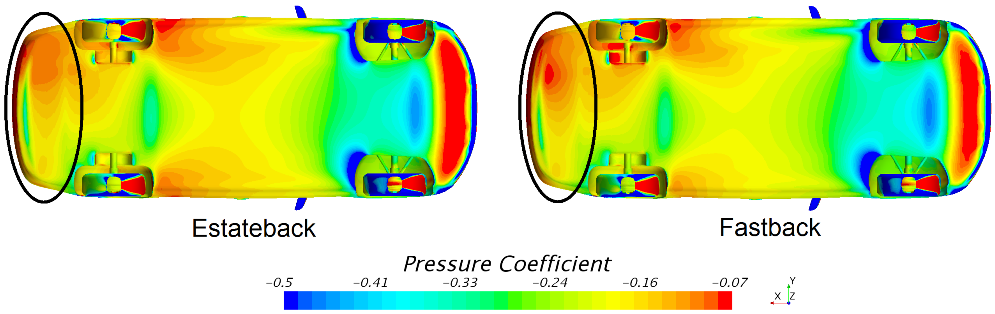


**Figure 8.8:** Pressure coefficient of the underbody of the baseline models.

According to the baseline results together with benchmarking, the guiding vanes were created. To reduce the number of varying parameters to only one, a starting location and a fixed width and height was set for all cases. The only varying parameter is the length of the vanes as shown in figure 8.9.

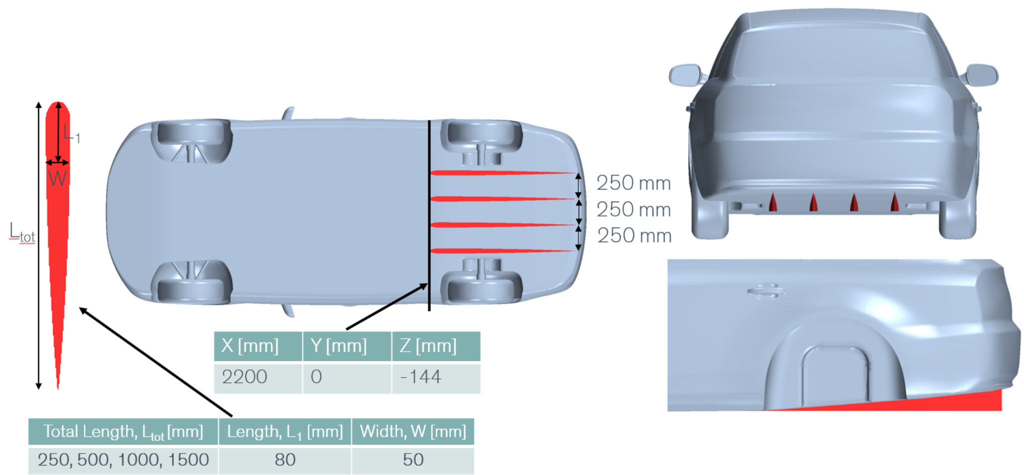


**Figure 8.9:** Design parameters of the underbody vanes concept

Four different cases with the lengths 250mm, 500mm, 1000mm and 1500mm are to be investigated. The starting point of the vanes is set when the flow deviation starts to be significant (shown as x,y,z coordinates in the figure) while the width is set to 50mm and the height of the vanes are following the flat underbody panel (not considering the diffuser).

## 8.5 Diffuser Extension

The design parameters of the diffuser extension are based on the benchmarking and literature studies. The diffuser angle of the DrivAer model is not changed due to it being around 5° which corresponds to a high level of drag reduction according to the results obtained by Löfdahl's study of different diffuser angles and their drag reducing abilities.

The width of the diffuser extension is set to correspond to the width between the rear tires. Three different length of the extensions are decided to be studied: 200mm, 300mm and 400mm. In figure 8.10, the design of the diffuser extension concept is shown.

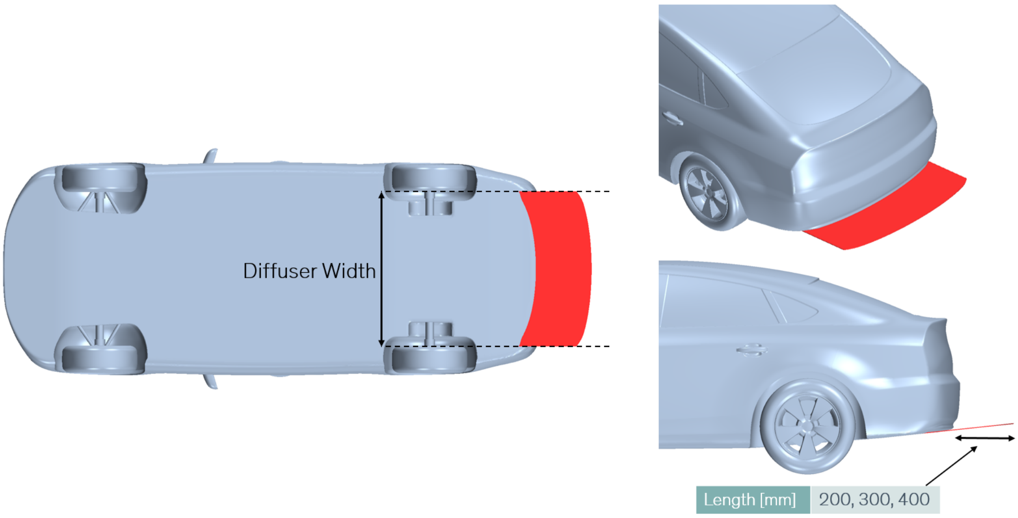


**Figure 8.10:** The concept design parameters of the diffuser extensions

## 8.6 Roof and Trunk Spoiler Extension

The roof and trunk spoiler extensions are designed in the same way as the diffuser extensions hence by literature studies and benchmarking results. For each vehicle configuration, three extensions: 100mm, 200mm and 300mm are created. Both the roof spoiler extension and trunk spoiler extension are following the vehicle curvature as shown in figures 8.11 and 8.12.

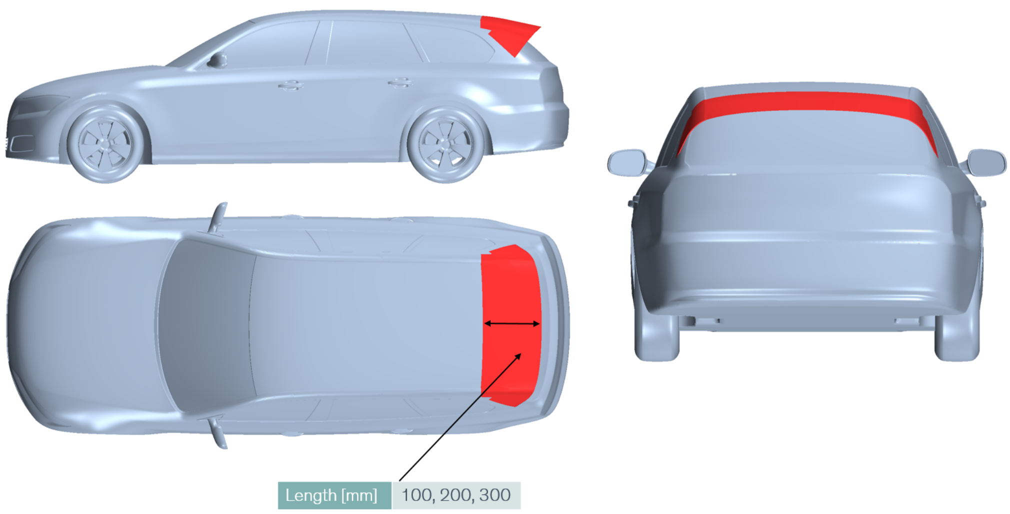


**Figure 8.11:** Design parameters of the roof spoiler extension concept.

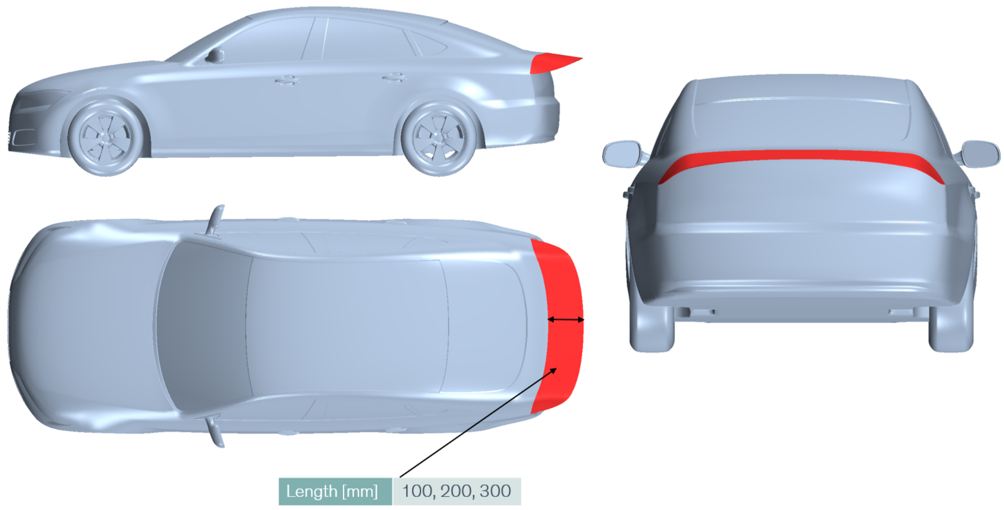


**Figure 8.12:** Design parameters of the trunk spoiler extension concept.

# 9
# Results

## 9.1 Air Curtain

In table 9.1, the results for the air curtain compared to the baseline model for both the estateback and the fastback configuration are shown. A drag reduction is obtained in the majority of the cases with a similar behaviour between the different configurations. The largest drag reduction for the estateback is obtained with the 10 mm concept and gives a 6 count reduction while for the fastback it is the 20mm concept with a drag reduction of 7 counts.

**Table 9.1:** Baseline vs air curtain results for the two vehicle configurations.

Estateback

| Configuration | Frontal Area [m²] | Cd | CdA | ΔCd [Counts] | ΔCdA [%] |
|---|---|---|---|---|---|
| Baseline | 2,162 | 0,271 | 0,586 | REF | |
| 10 mm | 2,162 | 0,265 | 0,573 | -6 | -2,2 |
| 20 mm | 2,162 | 0,268 | 0,579 | -3 | -1,1 |
| 30 mm | 2,162 | 0,269 | 0,582 | -2 | -0,7 |

Fastback

| Configuration | Frontal Area [m²] | Cd | CdA | ΔCd [Counts] | ΔCdA [%] |
|---|---|---|---|---|---|
| Baseline | 2,158 | 0,249 | 0,537 | REF | |
| 10 mm | 2,158 | 0,243 | 0,524 | -6 | -2,4 |
| 20 mm | 2,158 | 0,242 | 0,522 | -7 | -2,8 |
| 30 mm | 2,158 | 0,247 | 0,533 | -2 | -0,8 |

In figure 9.1, the pressure distribution on the wheel for both the baseline and the 10 mm concept simulation are shown. Looking inside the highlighted areas, the pressure coefficient have been reduced at the front part of the tire for the concept simulation. This result indicates that the flow velocity past the tire is increased. The air curtain feature have accelerated the airflow which have resulted in a reduction of drag.

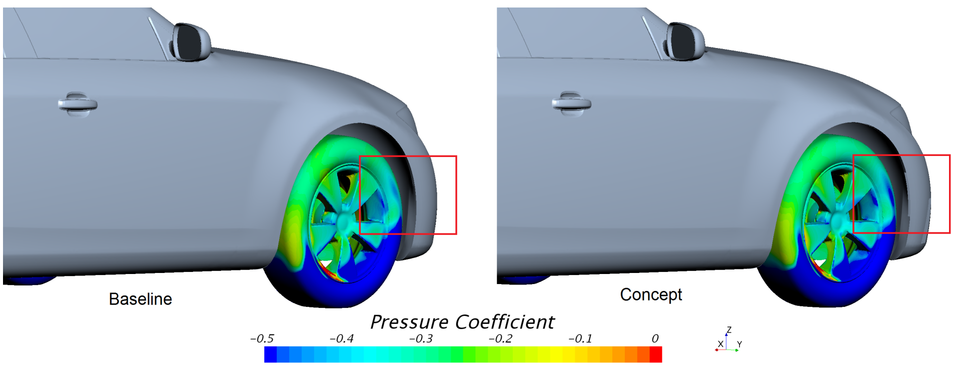


**Figure 9.1:** Pressure distribution tire, baseline vs air curtain concept

Creating a plane section at 100mm in z-direction, the velocity magnitude of the airflow is visualized, as shown in figure 9.2. In the concept case, the air flow past the outer edge of the tire and past the wheelhouse is more attached to the vehicle surface than for the baseline case.

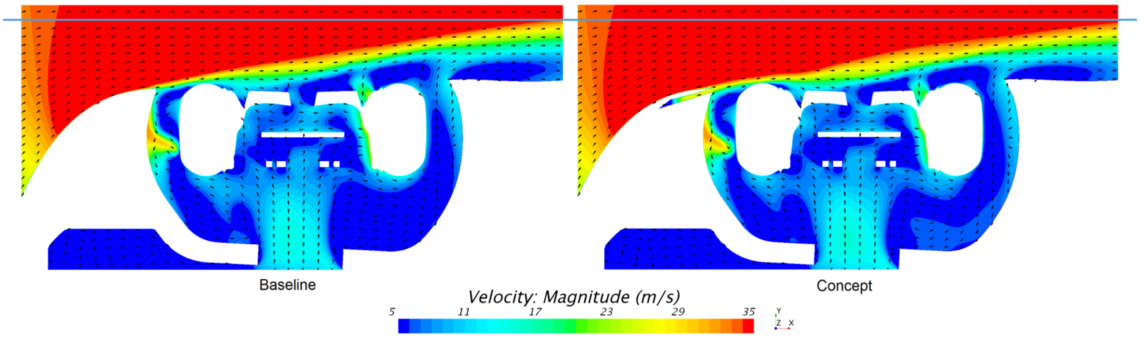


**Figure 9.2:** Comparison of the velocity magnitude between the baseline model and the concept at z-direction:+100mm

In the same figure, the velocity direction is visualized with vectors in order to follow the change in airflow direction. Due to the fact that the engince bay outlet is located in the wheelhouses, the exiting airflow of the engine bay is disturbing the air flow past the front tire and wheelhouse.

## 9.2 Wheelhouse Ventilation

In table 9.2, the results for wheelhouse ventilation concepts and baseline model is shown. This is done for both the estateback and fastback configuration. Implementing the concepts to the estateback, a drag reduction of 4-6 counts is obtained. In the fastback the drag reduction is between 1-3 counts which corresponds to almost 50% less drag reduction compared to the estateback.

**Table 9.2:** Baseline vs wheelhouse ventilation results for the two vehicle configurations.

Estateback

| Configuration | Frontal Area [m²] | Cd | CdA | ΔCd [Counts] | ΔCdA [%] |
|---|---|---|---|---|---|
| Baseline | 2,162 | 0,271 | 0,586 | REF | |
| 100 mm | 2,162 | 0,265 | 0,573 | -6 | -2,2 |
| 200 mm | 2,162 | 0,266 | 0,575 | -5 | -1,8 |
| 300 mm | 2,162 | 0,265 | 0,573 | -6 | -2,2 |
| 400 mm | 2,162 | 0,267 | 0,577 | -4 | -1,5 |

Fastback

| Configuration | Frontal Area [m²] | Cd | CdA | ΔCd [Counts] | ΔCdA [%] |
|---|---|---|---|---|---|
| Baseline | 2,158 | 0,249 | 0,537 | REF | |
| 100 mm | 2,158 | 0,246 | 0,531 | -3 | -1,2 |
| 200 mm | 2,158 | 0,248 | 0,535 | -1 | -0,4 |
| 300 mm | 2,158 | 0,246 | 0,531 | -3 | -1,2 |
| 400 mm | 2,158 | 0,247 | 0,533 | -2 | -0,8 |

Looking at the correlation between the configurations, it is shown that the concepts with 100mm and 300mm wheelhouse ventilation opening gives the largest drag reduction. In figure 9.3, a ZY-plane cut is made to show the pressure distribution in the rear part of the wheelhouse (highlighted surfaces). The baseline model gives a high pressure area in the rear part of the wheelhouse due to it acting as a "wall" in which the air flow hits due to not having an easy exiting path. The flow have two ways out of the wheelhouse, one is exiting to the sides (in positive/negative Y-direction) or under the vehicle (negative Z-direction). In this case the flow will still always hit the rear part of the wheelhouse. Implementing the wheelhouse ventilation opening the air flow have a third exiting path (positive X-direction). This path gives a reduction in the pressure coefficient at the rear part of the wheelhouse due to the "wall" having an opening where the flow can exit hence reducing the air flow exiting in other directions.

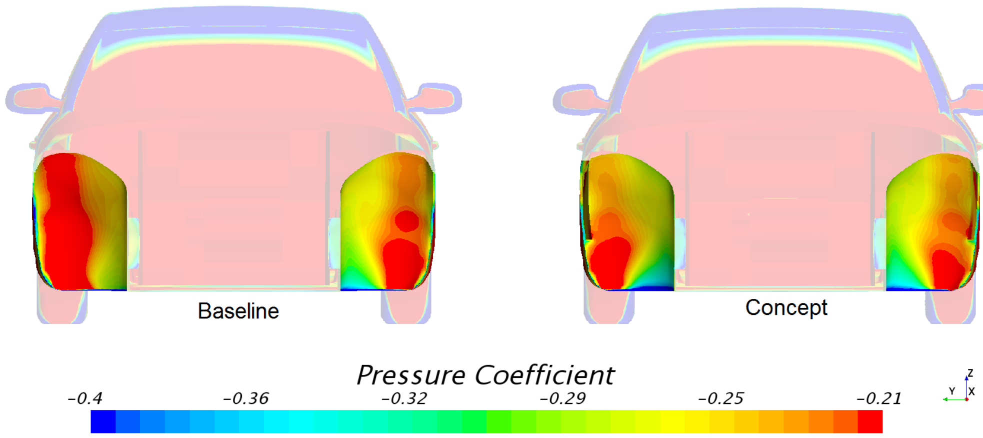


**Figure 9.3:** Pressure distribution in wheelhouse, baseline vs 300mm concept.

In figure 9.4, it is clearly noticeable that the overall pressure inside the wheelhouse is reduced. That indicates that more air flow is exiting the wheelhouse than in the baseline model. Looking at the rear edge of the wheelhouse arch, the pressure is increased which is a result of a more attached flow. Giving the wheelhouse ventilation opening, it have redirected the flow from exiting to the sides (positive/negative Y-direction) to exiting through the wheelhouse ventilation opening. This reduces the separation occuring at the rear wheelhouse arc hence allowing for a more surface attached flow which results in lowering the Cd.

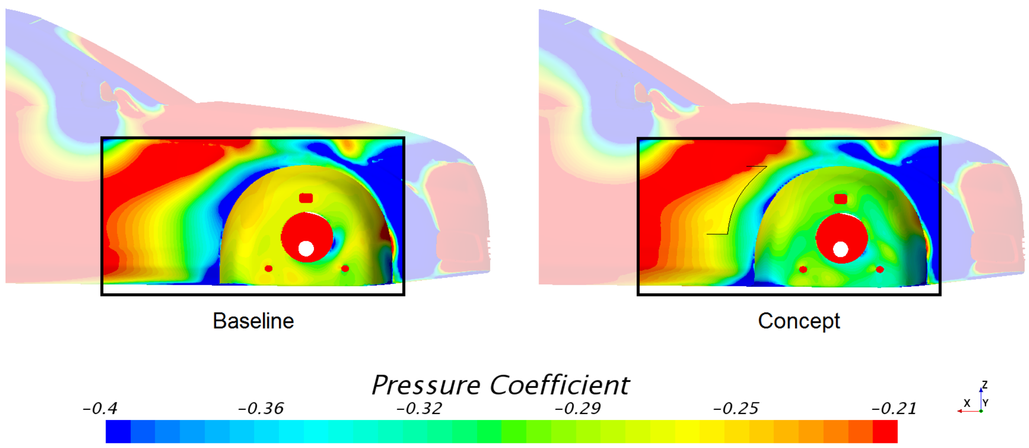


**Figure 9.4:** Pressure distribution wheelhouse, baseline vs 300mm concept.

As the air flow follows the car geometry from front-end to rear-end, all flow deviations and flow behaviours are resulting in a base wake. In this case the base wakes of both the estateback and fastback configurations are shown in figure 9.5. The change in base wake size from baseline to concept is not noticeably large. For the upper section of the vehicles, the base wake keeps the same but for the lower section the base wake is slightly reduced resulting in higher pressure at the rear-end giving a higher drag reduction.

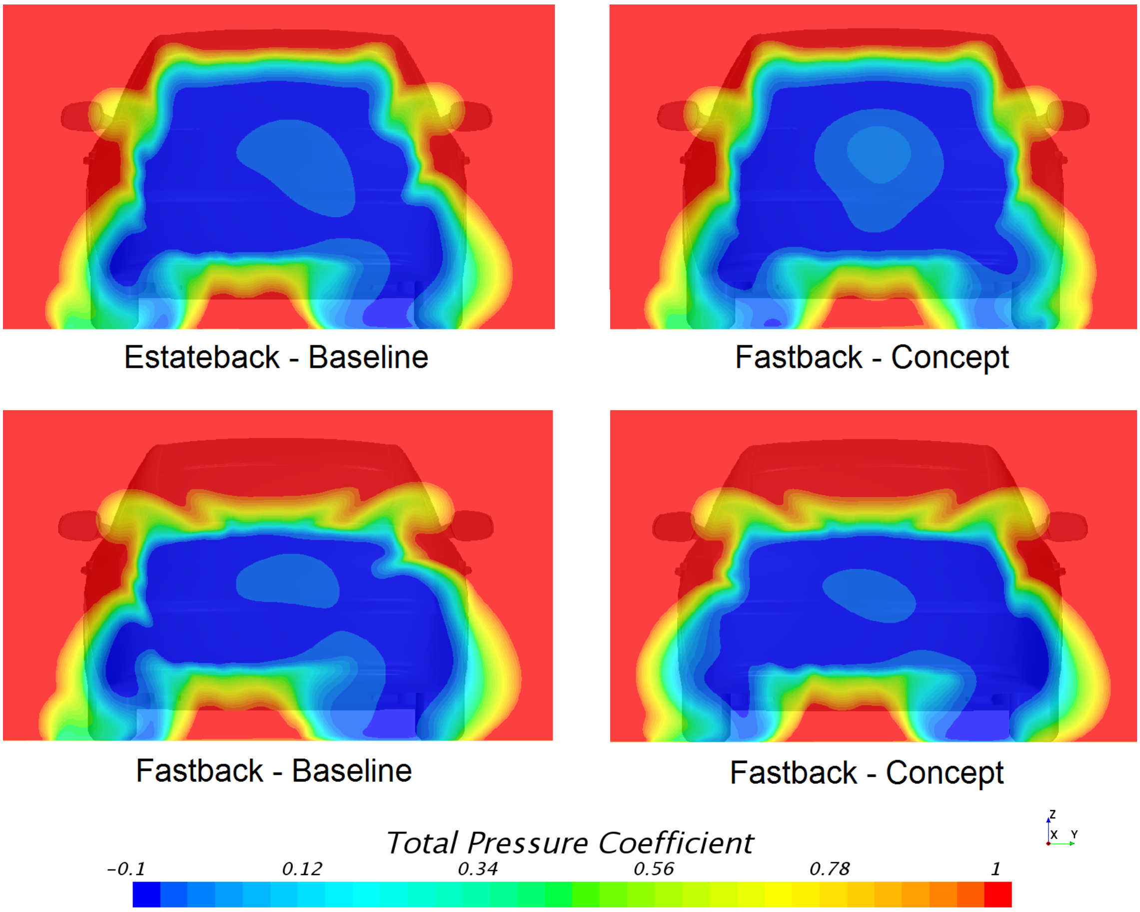


**Figure 9.5:** Base wake for both vehicle configurations taken 100 mm behind of the vehicle.

## 9.3 Front Spoiler/Splitter Package

A front spoiler/splitter package increases the frontal area of vehicles in which a reduction of the total drag might not be possible when considering the frontal area together with the Cd value. In table 9.3, the results for the front spoiler/splitter packages together with the baseline and both the vehicle configurations are shown. The Cd values for the different cases are based on the frontal area of the baseline in order to make the comparison of the results reliable.

**Table 9.3:** Baseline vs spoiler/splitter results for the two vehicle configurations.

Estateback

| Configuration | Frontal Area [m²] | Cd | CdA | ΔCd [Counts] | ΔCdA [%] |
|---|---|---|---|---|---|
| Baseline | 2,162 | 0,271 | 0,586 | REF | |
| 40 mm | 2,162 | 0,289 | 0,625 | 18 | 6,6 |
| 80 mm | 2,199 | 0,290 | 0,638 | 19 | 8,8 |
| 120 mm | 2,250 | 0,266 | 0,599 | -5 | 2,2 |

Fastback

| Configuration | Frontal Area [m²] | Cd | CdA | ΔCd [Counts] | ΔCdA [%] |
|---|---|---|---|---|---|
| Baseline | 2,158 | 0,249 | 0,537 | REF | |
| 40 mm | 2,158 | 0,263 | 0,568 | 14 | 5,6 |
| 80 mm | 2,199 | 0,265 | 0,583 | 16 | 8,4 |
| 120 mm | 2,246 | 0,251 | 0,564 | 2 | 4,9 |

The table shows that only the 120 mm case in the estateback configuration reduced the drag coefficient. The drag reduction is 5 counts. For both configurations, the same trend between the cases is obtained showing that a front spoiler/splitter of 40 mm gave more reduction than a length of 80mm followed. This is followed by the 120mm case which is giving the largest reduction between the cases. When considering the CdA values, it is shown that when taken the frontal area of the different cases into account, no drag reduction is obtained.

Looking at the accumulated drag along the estateback configuration, figure 9.6, it is shown that for the drag reducing concept, the majority of the difference comes from the front-end. At the front-end, a higher amount of drag is produced compared to the baseline as a result of a larger frontal area. At X=1250mm the drag cofficient drops drastically compared to the baseline. The difference in drag coefficient between the baseline and concept is not significant along the rest of the vehicle. At the rear of the vehicle however, the drag coefficient differs as a result of adding the drag coefficient along the vehicle.

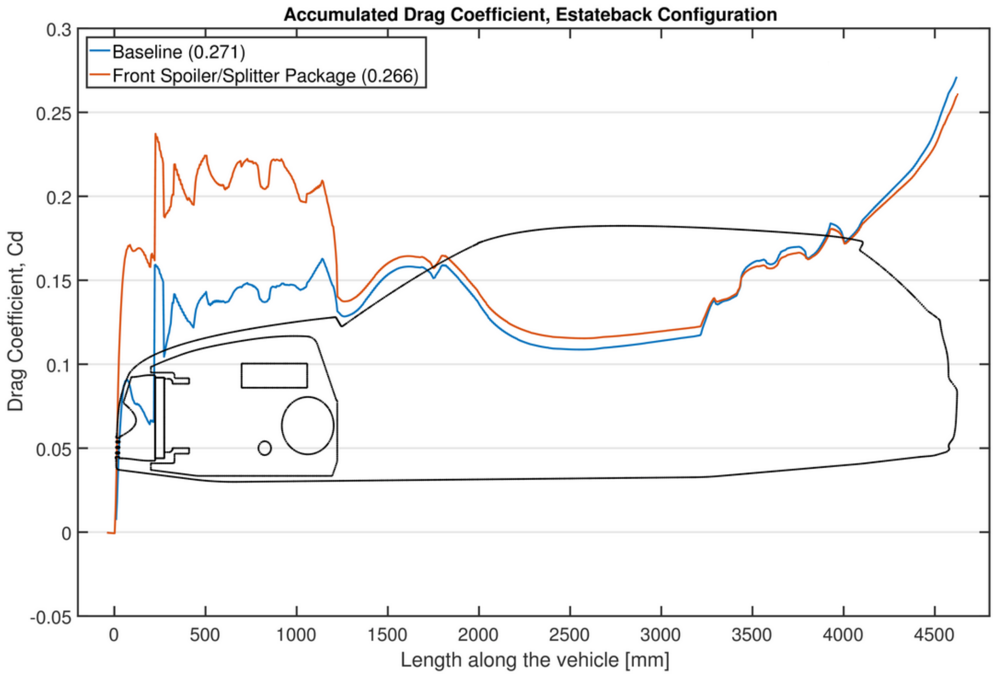


**Figure 9.6:** Accumulated drag along the vehicle length for the estateback

In figure 9.7, it is shown that with the front spoiler/splitter package it covers the tires which results in a reduction of front tire stagnation area. The stagnation is transerred to the front spoiler.

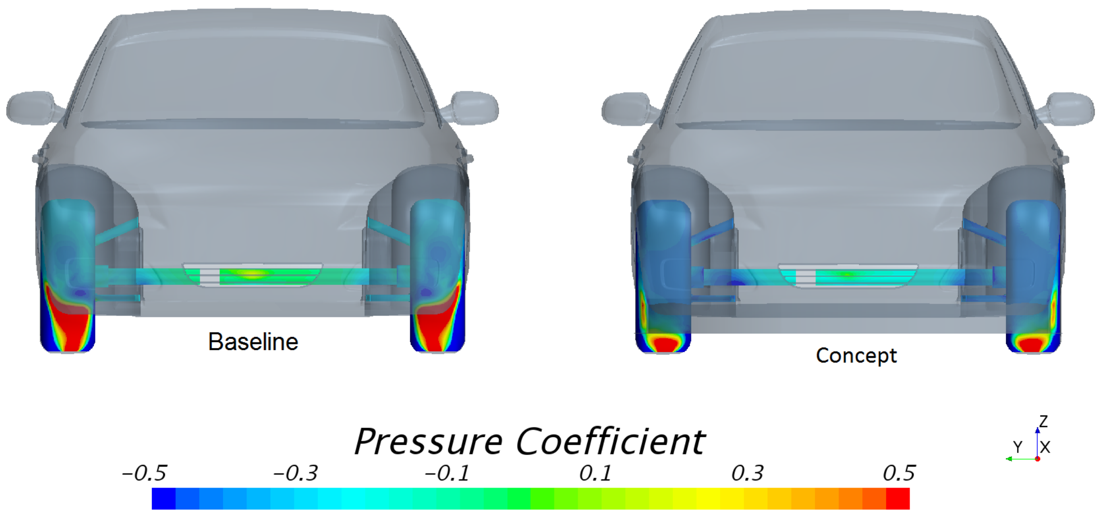


**Figure 9.7:** Tire stagnation area baseline vs the 120mm concept

With the use of a splitter together with the spoiler, the main airflow is redirected from passing under the vehicle (negative z-direction) to passing on the sides (positive/negative Y-direction). The airflow which are passing under the splitter and in under the vehicle is accelerated due to the low clearance between splitter and ground. In figure 9.8, it is shown that the pressure coefficient is lower in the wheelhouse area for the concept compared to the baseline. This is the result of the high speed flow velocity both past the side and under the wheelhouse hence creating a low pressure area in the wheelhouse.

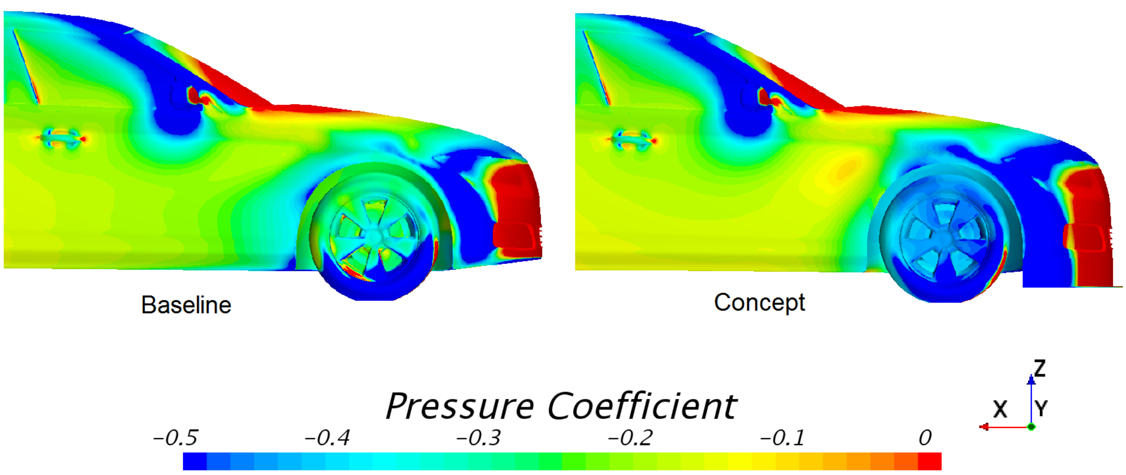


**Figure 9.8:** Pressure distribution wheelhouse, baseline vs spoiler/splitter concept.

An interesting result is when looking inside the engine bay shown in figure 9.9. The pressure coefficient is overall reduced with the front spoiler/splitter package. As the only outlets for the engine bay are in the wheelhouses, the high pressure inside the engine bay together with the low pressure of the air flow past the side and under the wheelhouse have created a suction effect in which the airflow is directed from the high pressure area to the low pressure area.

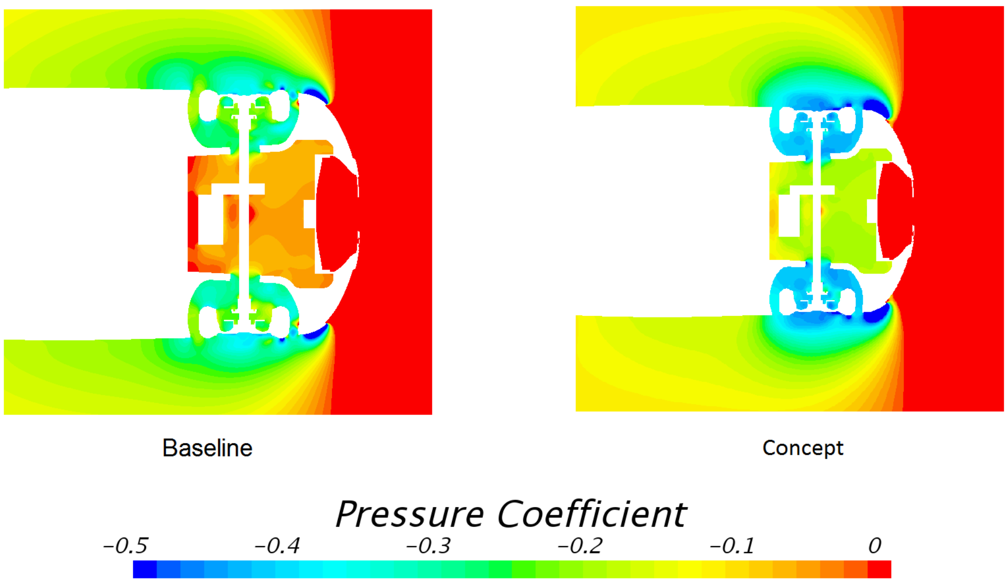


**Figure 9.9:** Pressure distribution engine-bay, baseline vs spoiler/splitter concept.

The drag produced by the high stagnation area in front of the vehicle is counteracted by the reduction of pressure coefficient in the engine bay which lead to a drag reduction. This behaviour correlates to what is seen in figure 9.6

## 9.4 Underbody Vanes

As shown in table 9.4, the use of underbody vanes results in drag reductions. However, for the different configurations, different amount of drag reduction is obtained.

**Table 9.4:** Baseline vs underbody vanes results for the two vehicle configurations.

Estateback

| Configuration | Frontal Area [m²] | Cd | CdA | ΔCd [Counts] | ΔCdA [%] |
|---|---|---|---|---|---|
| Baseline | 2,162 | 0,271 | 0,586 | REF | |
| 250 mm | 2,162 | 0,265 | 0,573 | -6 | -2,2 |
| 500 mm | 2,162 | 0,267 | 0,577 | -4 | -1,5 |
| 1000 mm | 2,162 | 0,270 | 0,584 | -1 | -0,4 |
| 1500 mm | 2,162 | 0,273 | 0,590 | 2 | 0,7 |

Fastback

| Configuration | Frontal Area [m²] | Cd | CdA | ΔCd [Counts] | ΔCdA [%] |
|---|---|---|---|---|---|
| Baseline | 2,158 | 0,249 | 0,537 | REF | |
| 250 mm | 2,158 | 0,244 | 0,527 | -5 | -2,0 |
| 500 mm | 2,158 | 0,244 | 0,527 | -5 | -2,0 |
| 1000 mm | 2,158 | 0,244 | 0,527 | -5 | -2,0 |
| 1500 mm | 2,158 | 0,248 | 0,535 | -1 | -0,4 |

The estateback obtained the largest drag reduction with the 250 mm vanes corresponding to 6 counts. A trend is found for the estateback and the longer the vanes becomes, the less drag is reduced. In the 1500mm case the drag is instead increased. For the fastback, the results differ compared to the estateback. The 250 mm, 500mm and 1000mm results give the same drag reduction corresponding to 5 counts. For the 1500mm case, the drag is reduced by only 1 count.

In figure 9.10, the streamlines are showing how the flow is distributed along the underbody with the use of the vanes. The 1500mm vanes resulted in the most uniformed flow, following the underbody panel with no big deviations in y-direction. Compared to the baseline run results, all lengths of the vanes resulted in a more uniform flow distribution. However, for the estateback, the drag coefficient is increased the longer the vanes are, and for the fastback, same behaviour is noticed even though the drag coefficient shows the same for three different lengths.

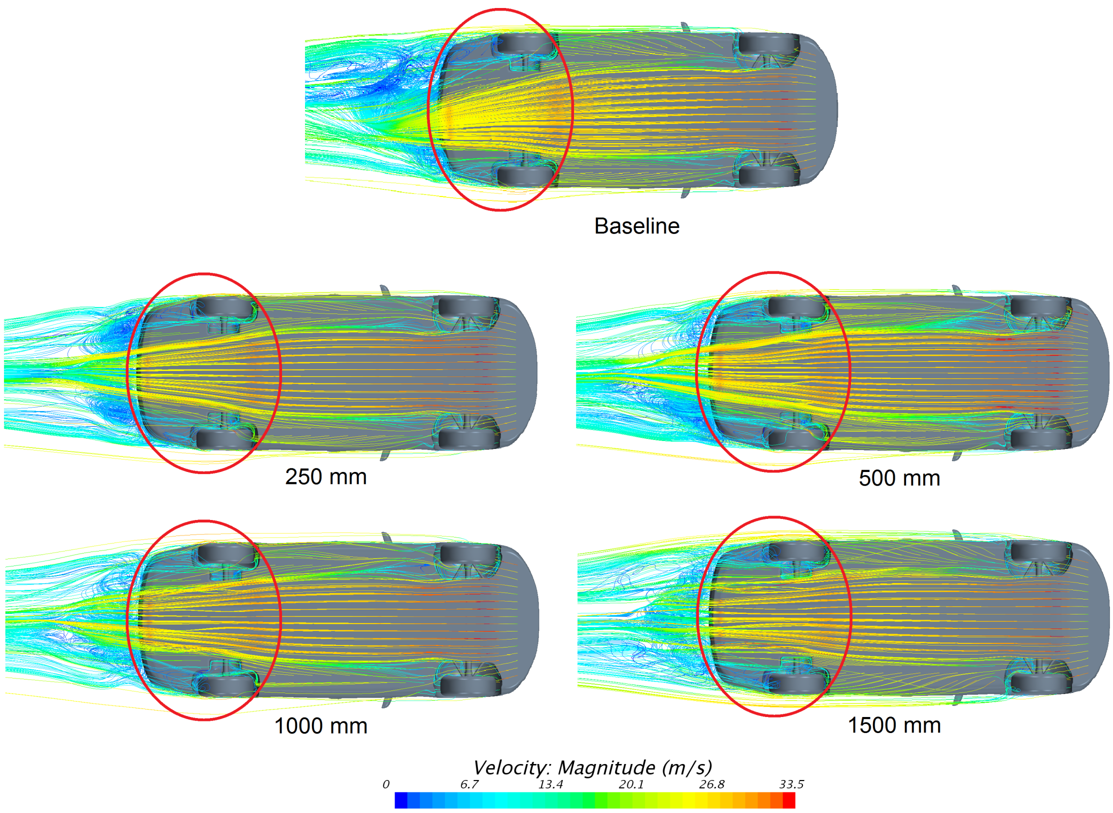


**Figure 9.10:** Distribution of the underbody flow for the different vane lengths.

## 9.5 Diffuser Extension

With a diffuser extension feature, a drag reduction of 3-9 counts for the estateback and 3-8 counts for the fastback is obtained as shown in table 9.5. The results between the estateback and fastback are inverted thus the best case for the estateback is the 200mm extension and for the fastback the 400mm is the best case.

**Table 9.5:** Baseline vs diffuser extension results for the two vehicle configurations.

Estateback

| Configuration | Frontal Area [m²] | Cd | CdA | ΔCd [Counts] | ΔCdA [%] |
|---|---|---|---|---|---|
| Baseline | 2,162 | 0,271 | 0,586 | REF | |
| 200 mm | 2,162 | 0,262 | 0,566 | -9 | -3,3 |
| 300 mm | 2,162 | 0,267 | 0,577 | -4 | -1,5 |
| 400 mm | 2,162 | 0,268 | 0,579 | -3 | -1,1 |

Fastback

| Configuration | Frontal Area [m²] | Cd | CdA | ΔCd [Counts] | ΔCdA [%] |
|---|---|---|---|---|---|
| Baseline | 2,158 | 0,249 | 0,537 | REF | |
| 200 mm | 2,158 | 0,246 | 0,531 | -3 | -1,2 |
| 300 mm | 2,158 | 0,244 | 0,527 | -5 | -2,0 |
| 400 mm | 2,158 | 0,241 | 0,520 | -8 | -3,2 |

In figure 9.11, the pressure coefficient distribution along the center of the estateback is shown. Compared to the baseline it is seen that the base pressure of the vehicle is increased in all cases. This explains the drag reduction with the use of a diffuser extension.

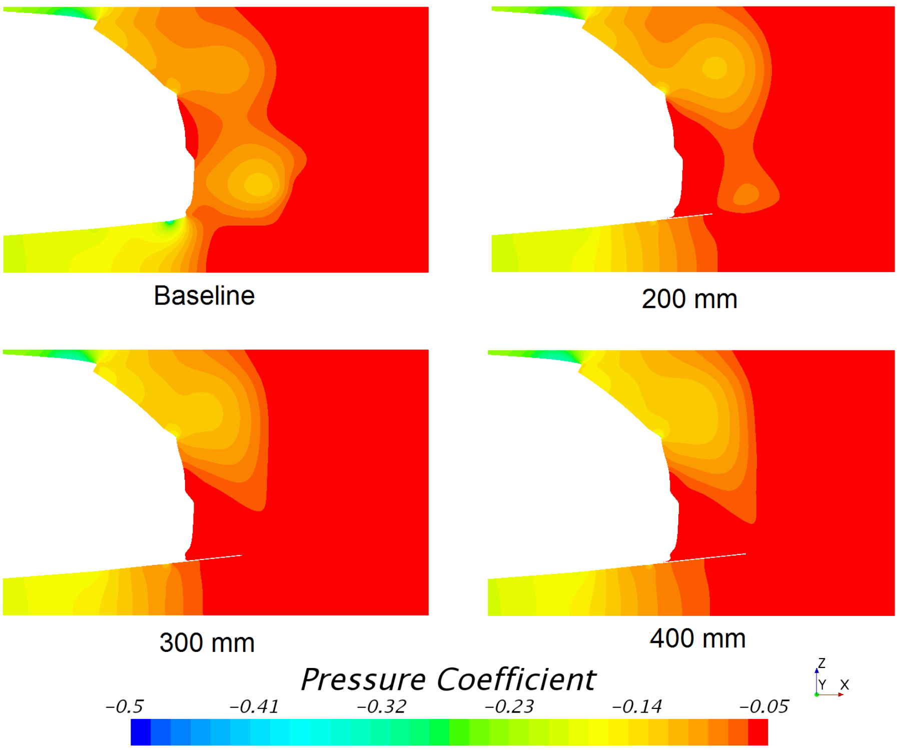


**Figure 9.11:** Pressure distribution along the center of the estateback.

To understand why the 200mm resulted in the largest drag reduction followed by the 300mm and the 400mm cases for the estateback configuration, the airflow streamlines along the center of the vehicle are visualized as shown in figure 9.12. As seen for the baseline model, it has a two longitudinal vortex structure which is originating from the roof and underbody. With a 200mm diffuser extension, the lower vortex is delayed and becomes smaller compared to the baseline model. For the 300mm and 400mm diffuser extensions, the lower vortex almost disappears, however making the upper vortex structure bigger. As shown in figure 9.11, the 300 mm and 400 mm have a lower pressure at the rear window compared to the 200mm case which is due to the upper vortex getting bigger.

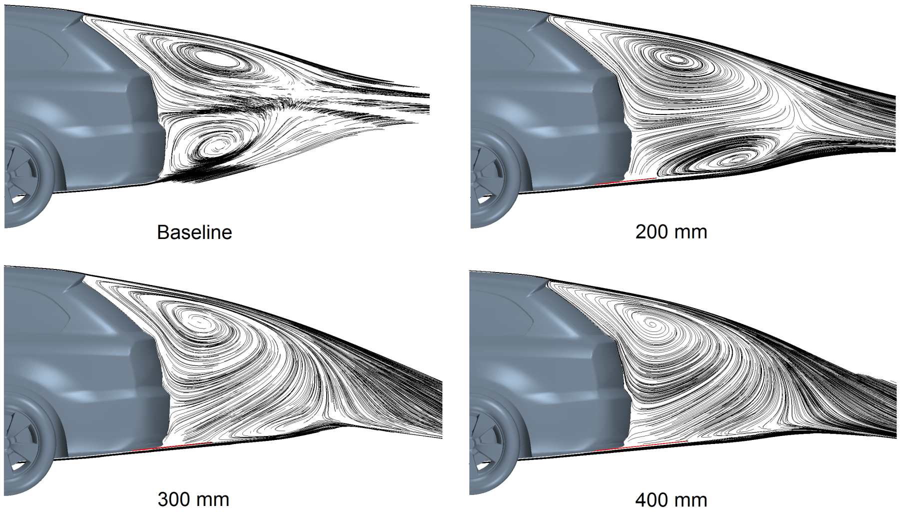


**Figure 9.12:** Streamlines along the center of the estateback.

For the fastback configuration, a longer extension gives a lower drag. In figure 9.13, a cut plane along the center of the vehicle shows the pressure coefficient distribution. It is seen that, as for the estateback, an extension of the diffuser gives an increase of the base pressure at the rear-end compared to the baseline model. The largest increase of base pressure is obtained with the 400mm case and hence resulting in the largest drag reduction.

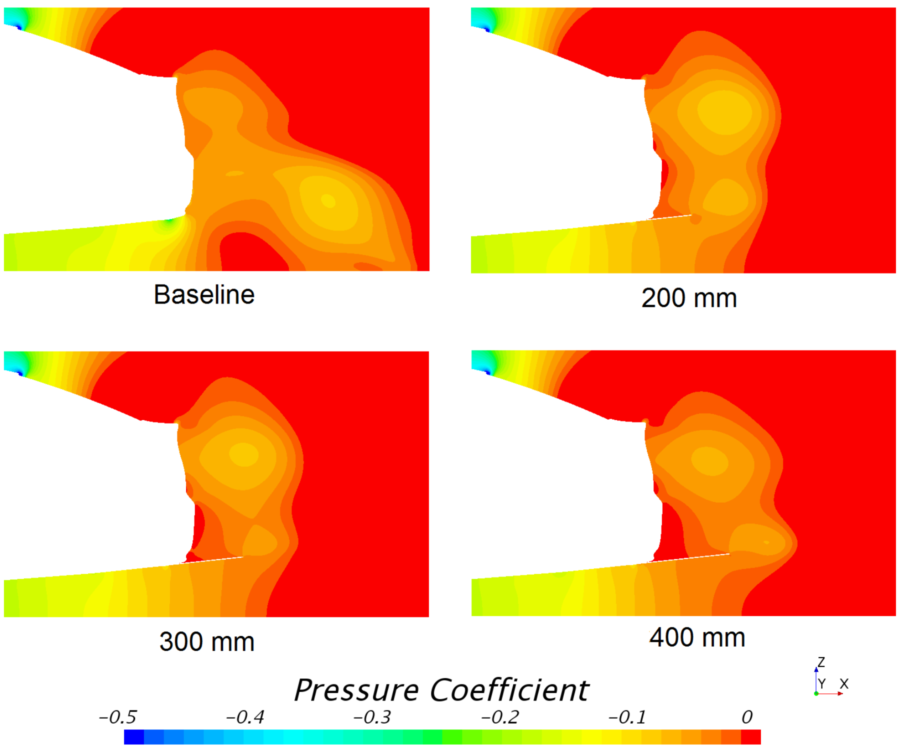


**Figure 9.13:** Pressure distribution along the center of the fastback.

In figure 9.14, the airflow streamlines along the center of the fastback is shown. As for the estateback, the baseline model have two big vortices at the rear-end. As the lower vortex become smaller and the separation is delayed, the result is an increased base pressure and a reduction of the drag coefficient.

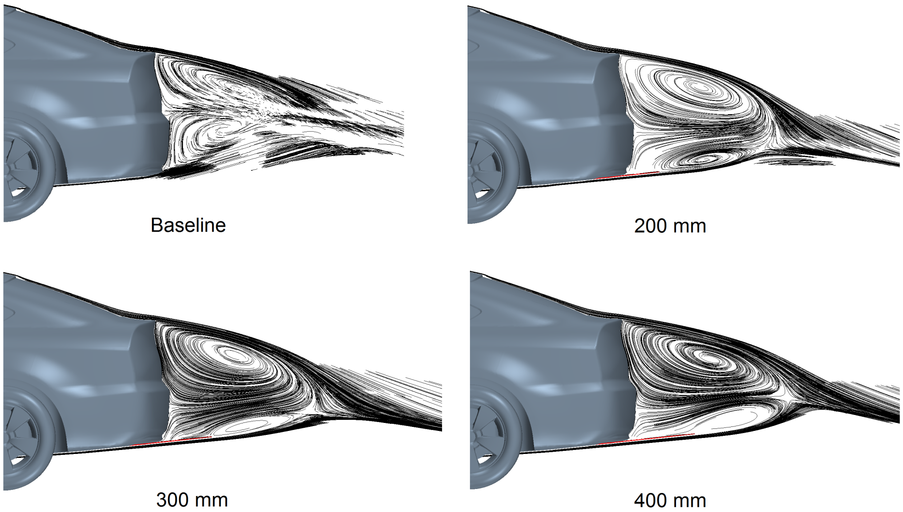


**Figure 9.14:** Streamlines along the center of the fastback.

## 9.6 Roof/Trunk Extension

In table 9.6, the estateback roof spoiler extension concept and the fastback trunk spoiler extension concept together with the baseline model are presented. For the estateback, the 100mm of roof spoiler extension gave the same result as the baseline model. With the 200mm roof spoiler extension, a drag reduction of 4 counts is obtained while for the 300mm roof spoiler extension a drag reduction of 8 counts is obtained. These results shows that for the estateback, a longer roof spoiler tends to reduce the most drag. For the fastback configuration the drag reduction is similar to the estateback hence a drag reduction of 4-9 counts is obtained. Opposite to the estateback configuration, the shortest extension, 100mm gave the best result followed by the 200mm and the 300mm cases.

**Table 9.6:** Baseline vs roof/trunk spoiler extension results

Estateback

| Configuration | Frontal Area [m²] | Cd | CdA | ΔCd [Counts] | ΔCdA [%] |
|---|---|---|---|---|---|
| Baseline | 2,162 | 0,271 | 0,586 | REF | |
| 100 mm | 2,162 | 0,271 | 0,586 | 0 | 0,0 |
| 200 mm | 2,162 | 0,267 | 0,577 | -4 | -1,5 |
| 300 mm | 2,162 | 0,263 | 0,569 | -8 | -3,0 |

Fastback

| Configuration | Frontal Area [m²] | Cd | CdA | ΔCd [Counts] | ΔCdA [%] |
|---|---|---|---|---|---|
| Baseline | 2,158 | 0,249 | 0,537 | REF | |
| 100 mm | 2,158 | 0,240 | 0,518 | -9 | -3,6 |
| 200 mm | 2,158 | 0,245 | 0,529 | -4 | -1,6 |
| 300 mm | 2,158 | 0,242 | 0,522 | -7 | -2,8 |

In figure 9.15 it is clearly seen that the rear wake differs between the baseline and 300mm roof extension concept. For the 300mm roof extension concept, the flow velocity at the rear-end is smaller than for the baseline case. This results in a higher base pressure recovery and hence a smaller wake size with a drag reduction of 8 counts compared to the baseline model.

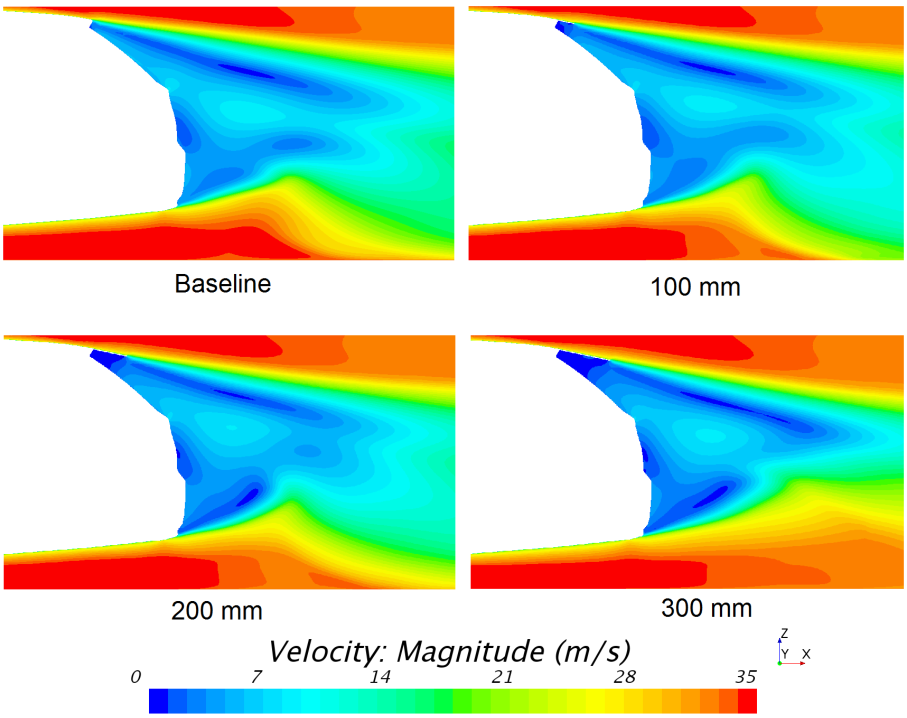


**Figure 9.15:** Velocity magnitude along the center of the estateback.

In figure 9.16, the airflow streamlines along the center of the estateback is shown. It can be seen using a roof extension, the upper vortex is delayed and hence, as for the diffuser extension concepts, reducing the drag coefficient.

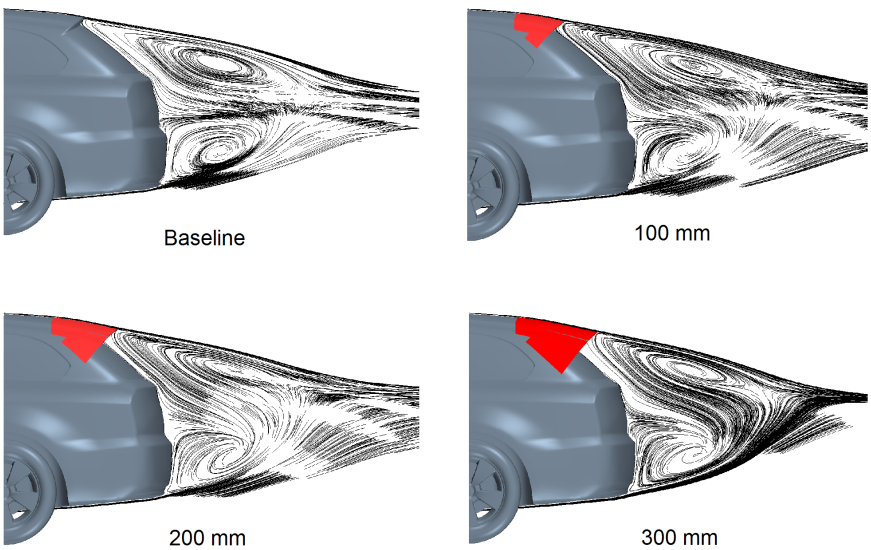


**Figure 9.16:** Streamlines along the center of the fastback.

For the fastback configuration, the pressure coefficient at the rear-end for the different trunk spoiler extensions are shown in figure 9.17. The differences in base pressure recovery between baseline and the different concepts are easily noticed. The 100 mm trunk spoiler extension results in the lowest wake size of the cases and hence gives the largest drag reduction which corresponds to 9 counts.

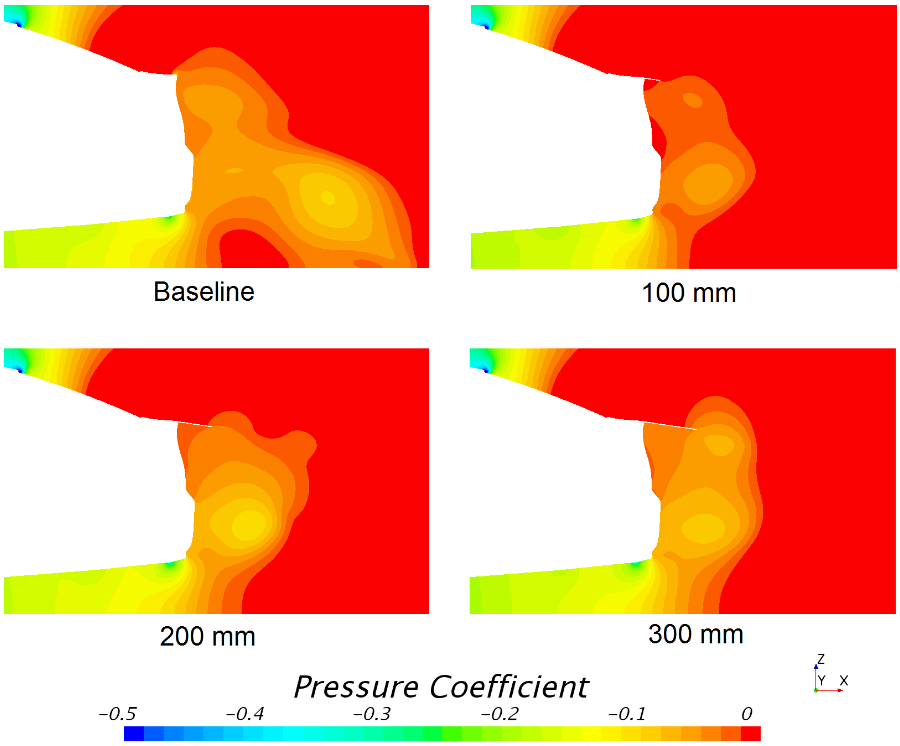


**Figure 9.17:** Pressure distribution along the center of the fastback.

## 9.7 Combined and Futuristic Concept Configuration

In order to evaluate the combined aerodynamic performance of the concepts, the best case in each concept for both the estateback and fastback configuration was combined in the DrivAer model and simulated.

Starting with the estateback, a 10mm air curtain, a 300mm wheelhouse ventilation, 250mm underbody vanes, a 200mm diffuser extension and a 300mm roof extension was combined and simulated. For the fastback a 10mm air curtain, a 300mm wheelhouse ventilation, 250mm underbody vanes, a 400mm diffuser extension and a 100mm trunk extension are are combined and simulated. The front spoiler/splitter package was not used due to it not reducing the total drag.

Additional to the combined concept configuration, one further step is taken in order to create a futuristic concept configuration. This configuration is based on the combined concept configuration but with additional features such as a closed grille, removed side mirrors and no door handles. The idea to simulate a futuristic concept configuration is risen to give an insight in a futuristic aerodynamically design of era.

The results of these concepts are presented in table 9.7. For the estateback a drag reduction of 15 counts is obtained with the combined concept configuration. The change in CdA value is 5.5% which results in an increase in the range for an electric vehicle. Looking at the futuristic concept configuration of the estateback, a drag reduction of 35 counts is obtained which corresponds to more than 50% improvement. With the futuristic concept, the frontal area drops from 2.162 $m^2$ to 2.106 $m^2$, thus significantly reducing the CdA value by 15.2%.

For the fastback, the combined concept configuration did not give the same significant drag reduction as for the estateback. The drag reduction was only 5 counts. The futuristic concept however, reduced the drag by 33 counts and the CdA value by 15.5%.

**Table 9.7:** The results of the combined and futuristic concept configuration.

Estateback

| Configuration | Frontal Area [m²] | Cd | CdA | ΔCd [Counts] | ΔCdA [%] |
|---|---|---|---|---|---|
| Baseline | 2,162 | 0,271 | 0,586 | REF | |
| Combined | 2,162 | 0,256 | 0,553 | -15 | -5,5 |
| Futuristic | 2,106 | 0,236 | 0,497 | -35 | -15,2 |

Fastback

| Configuration | Frontal Area [m²] | Cd | CdA | ΔCd [Counts] | ΔCdA [%] |
|---|---|---|---|---|---|
| Baseline | 2,158 | 0,249 | 0,537 | REF | |
| Combined | 2,158 | 0,244 | 0,527 | -5 | -2,0 |
| Futuristic | 2,101 | 0,216 | 0,454 | -33 | -15,5 |

# 10
# Discussion

The drag reduction obtained for the air curtain concepts was significant but due to no literatures or previous studies found, a comparison to a real life case is not possible. However, when postprocessing the results, no significant changes could be obtained. It seems that the air curtain have affected the flow path in a general way and thus creating a more surface attached flow. Due to the fact that the engine bay cooling flow exits are located in the wheelhouses, the high velocity of the exiting flow is interacting with the outer flow past the wheelhouse hence reducing the drag reduction capacity of the air curtain. During the benchmarking study, designs and placements of air curtains have been investigated and by comparing the findings with the DrivAer model, it is shown that the front-end design of the DrivAer model is not designed with the use of an air curtain in mind. When implementing features to a vehicle, the first step is to optimize the vehicle geometry and using different features to further improve the performance. This was not the case with the implementation of the air curtain to the DrivAer model.

For the wheelhouse ventilation concept, the results cannot, as for the air curtain, be compared to a literature or previous studies due to poor publications. The CFD results however, shows that significant amounts of drag can be reduced. An interesting behaviour between the cases is that the opening length of the wheelhouse ventilation did not give a noticeable change in the drag coefficient value. It seems that investigating in where to place the wheelhouse ventilation opening can result in a larger decrease of drag coefficient than focusing on the actual wheelhouse design. Another result worth highlighting is that the reason to the different magnitudes of drag reduction between the two configurations is due to the geometries. The only difference is at the rear upper-body where the estateback results in a larger wake size than the fastback hence giving a larger volume in which an aerodynamic feature can reduce.

The front spoiler/splitter package did not reduce the air resistance exerted on the vehicle even though one concept managed to reduce the drag coefficient. One reason for that is that a flat underbody is used for the DrivAer model. The flat underbody does not disturb the airflow, which can keep a constant high velocity along the underbody making the baseline setup already optimal. According to a paper found about the front spoiler/splitter package for an conventional vehicle with a complex underbody, a 20% drag reduction could be obtained. This can not be confirmed with this thesis where a drag coefficient reduction of only 1.88%, with no reduction in total air resistance is found.

Analyzing the trends of the different front spoiler/splitter cases, it is shown that with the increase of spoiler length the drag coefficient can both be reduced or increased. To create a front spoiler/splitter package which gives the best performance a thourough study must be made where spoiler lengths and shapes are studied. Other interesting results is that the pressure in the engine bay is reduced due to a suction effect occurring at the engine bay cooling flow outlet. This behaviour was not expected thus with a deeper study of where the flow hitting the front-end is directed, to the sides or under the wheelhouse, could result in further drag reduction and also influence the lift forces.

The underbody vanes, as seen in the literature review and in the benchmarking have different designs however all is used to guide and control the flow along the underbody. In order to create underbody vanes for the DrivAer model, the baseline results were analyzed. Unlike many vehicles using guiding vanes stretching from front part of the underbody to the end part, it is decided to only use guiding vanes in areas in which the flow was in need of a more uniform distribution. Since the DrivAer model have a flat underbody it is possible to reduces the drag coefficient with up to 6 drag counts. However, due to the effect of the different massflows along the sides of the vehicle, the performance of the guiding vanes is affected. The longest vanes which in theory should give the largest drag reduction resulted in giving the least drag reduction and for the estateback configuration increasing the drag coefficient. Through the shorter vanes, the flow is guided and separated but when flowing past the vane the flow is again interacted causing a reduction of the difference in massflow for right and left side. For the long vanes, the flow in right side and left side are kept apart resulting in a bigger impact on the wake of the vehicle due to the effect of the unsymmetry.

The diffuser extension simulations are done to give an insight of an active aerodynamic feature and its possibilities to reduce drag. Studying a paper investigating in this type of feature together with the benchmarking of diffuser lengths and angles resulted in the fact that a drag reduction of up to 20 drag counts can be obtained. The goals with this feature was to reduce the wake size behind the vehicle by delaying the rear-end separation. For both vehicle configurations this goals were fulfilled and a drag reduction of 3-9 drag counts is obtained. An interesting result is that the diffuser extension lengths did not give the same result for the estateback and fastback. For the estateback the shortest extension gave the most drag reduction which increases with diffuser length while for the fastback it is vice versa, the most drag is reduced with the longest configuration which increases the shorter the extension is. This is an indication that shows that many features do not give the same performance when transferred between vehicle models.

Same as for the diffuser extension, a roof and a trunk extension is also simulated to give an insight of an another active feature that can be used in the near future. Vehicle concepts such as the Mercedes IAA and the Audi E-tron Quattro, proves that it is possible to reduce drag with the usage of an active rear-end extension. Studied papers and benchmarked vehicles shows that with a roof extension a drag reduction of 10 counts can be obtained. A similar result, corresponding to a drag reduction of 8-9 counts, is obtained for the roof and trunk extensions in this thesis. The significant point is with a different vehicle model, the optimum reduction is not the same. The best result for the estateback is a 300mm roof extension while a 100mm extension is the most efficient for the fastback configuration. The amount of the reduction is up to 9 drag counts can defined as significant improvement for an aerodynamic performance. As mentioned in introduction for this study, concept design have not been optimized. It means that these trunk/roof extension concepts might be even more efficient with the right angle and design shape.

In order to give an estimate on how much drag reduction that could be obtained with all the best cases of each concepts, it is not accurate to add all the drag reductions. The concepts have due to this been combined together in both the estateback and fastback configuration. A drag reduction of 5 counts is obtained for the fastback configuration which is lower than the least of the best concept. This result shows that some concepts are not working efficiently when simulated together with other concepts. For the estateback configuration, a drag reduction of 15 drag counts is obtained making the combined concept vehicle giving the best drag reduction compared to the single concept drag reduction. It is clearly shown that these results might be reduced even more with an optimized concept design.

The concept study is ended with a futuristic concept vehicle simulation which is inspired from concept vehicles made by car manufacturers. Today the aerodynamically efficient concept vehicles have Cd values of around 0.19-0.22. The estateback and fastback configurations resulted in a drag reduction of 33-35 counts, landing a Cd value of 0.236 for the estateback and 0.216 for the fastback. Taking in consideration that the DrivAer model is a few years old compared to todays vehicle models, these results are very interesting.

# 11
# Conclusion

To conclude this study, the aerodynamic performance of today's vehicles have not yet reached its fully potential. With new technologies and innovations more and more aerodynamic features are implemented in the vehicle design as noticed in the benchmarking study. In recent years the active aerodynamic features are getting more popular as a result of cheaper hardware and the wide implementation of software in vehicles. This opens up for new types of aerodynamic features in order to control the airflow and hence reduce drag.

In this thesis, different aerodynamic features have been emphasized. It is found that with the use of different types of features the drag of a vehicle is significantly changed. This results in the reduction of energy losses and for electric vehicles, the increase of range.

The features which gave the largest drag reduction are the diffuser and roof/trunk spoiler extension concepts. These concepts have a big potential to be implemented on vehicles in the near future. As the diffuser and roof/trunk spoiler extensions are considered as active features, they are only enabled when required thus keeping the aesthetics and safety of the vehicle at high levels.

Although the concepts that were investigated in do not represent their fully aerodynamic potential, the main focus should be made in optimizing the vehicle geometry before designing and optimizing an aerodynamic feature.

Finally, the performance of aerodynamic features is only valid for the specific vehicle model it have been developed for. Transferring the feature to another vehicle model will in most cases not give the same performance and must be further studied for full efficiency.

# 12
# Future Work

The main recommendation for a further investigation of this thesis is to use a completely closed vehicle body when investigating in new concepts. A closed vehicle body do not correspond to a real life case where e.g. cooling flow is required but it reduces the disturbance of the airflow and hence increasing the possibility to obtain a highly accurate performance of the analyzed concept.

To continue the study of the aerodynamic drag reduction on electric vehicles, a deeper study of the concept design parameters is recommended in order to enhance the performance and the drag reduction ability.

# Bibliography


[1] Eurostat (2015). Energy&transport in figures. Luxembourg: European Union. Available at: ec.europa.eu/transport/facts-fundings/statistics/doc/2013/pocketbook2013.pdf (2017-06-03)

[2] Barnard, R., "Road Vehicle Aerodynamic Design, 3rd Ed," (St Albans, MechAero Publishing, 2009), 54, ISBN:978-09540734-7-3.

[3] Lohse-Busch, H., Duoba, M., Rask, E., Stutenberg, K. et al. (2013) "Ambient Temperature (20°F, 72°F and 95°F) Impact on Fuel and Energy Consumption for Several Conventional Vehicles, Hybrid and Plug-In Hybrid Electric Vehicles and Battery Electric Vehicle," SAE Int. doi:10.4271/2013-01-1462

[4] NEVS AB (2015) Annual Report. Ernst&Young AB Available at: https://www.nevs.com/media/filer_public/e1/67/e167ce93-99d2-4101-838a-8a6549169600/nevs-annual-report-2015.pdf. (2017-06-03)

[5] Palin, R., Johnston V., Johnson S., et al. (2012). The aerodynamic development of the Tesla Model S - Part 1: Overview", SAE Int. doi:10.4271/2012-01-0177.

[6] Marti, O., "Streamlining Applied to Automobiles", SAE Technical Paper 310002, 1931, doi: 10.4271/310002

[7] Brown, L. and Chase, H., "Streamlining - Up-to-date Facts and Developments," SAE Technical Paper 340014, 1934, doi: 10.4271/340014

[8] Hucho, W-H., "Aerodynamics of Road Vehicles", 4th edition, SAE International, Warrendale, PA, ISBN: 978-0-7680-0029-0, 1998.

[9] Breer, C. and Yanik, A.J., "The Birth of the Chrysler Corporation and Its Engineering Legancy." SAE International, Warrendale, PA, ISBN: 978-1-56091-524-9, 1995, doi: 10.4271/R-144

[10] Good, G.L, Johnson, C., Clough, B. and Lewis, R., "The Aesthetics of Low Drag Vehicles." SAE International, 2011, doi: 10.4271/2011-37-0016

[11] Hemmings Sports & Exotic Car.. 2006. Turbine Speed with Style. [ONLINE] Available at: https://www.hemmings.com/magazine/hsx/2006/01/Turbine-Speed-with-Style/1282048.html. [Accessed 25 April 2017].

[12] Google image library.

[13] Hucho, W., Janssen L. and Emmelmann, H., "The Optimization of Body Details-A Method for Reducing the Aerodynamic Drag of Road Vehicles," SAE Technical Paper 760185, 1976, doi: 10.4271/760185.

[14] Buchheim, R., Deutenbach, K. and Luckoff, H. "Neccessity and Premises for Reducing the Aerodynamic Drag of Future Passenger Cars," SAE Technical Paper 810185, 1981, doi: 10.4271/810185.

[15] Buchheim, R., Leie, B. The Development of the Audi 100 - A new Approach in Aerodynamic Passenger Car Design, Vehicle Aerodynamics Sysmposium organised by VW, Dec 02-03. 1982.

[16] Emmelmann, H-J., Berneburg, H., Schulze J., "The Aerodynamic Development of the Opel Calibra" SAE Paper 900317, SAE Congress 1990.

[17] Larminie J, Lowry J (2003). Electric Vehicle Technology Explained. 1st ed. Chichester: John Wiley&Sons Ltd

[18] Brooke, Lindsay (Nov 4, 2010) "Sweating the Body Details". Vehicle Electrification. SAE International. 2010-11-01. p. 39. [ONLINE] Available at: http://www.nxtbook.com/nxtbooks/sae/10EVSD1104/index.php?lre=1%3 A3131394433443637344442344144344633373441453033413937384646463337/38 [Accessed 05 May 2017].

[19] Tesla Inc.. 2017. Tesla Model S. [ONLINE] Available at: https://www.tesla.com/models. [Accessed 11 May 2017].

[20] Tesla Inc.. 2017. Tesla Model X. [ONLINE] Available at: https://www.tesla.com/modelx. [Accessed 11 May 2017].

[21] BMW Group. 2016. The new BMW 5 Series Sedan. [ONLINE] Available at: https://www.press.bmwgroup.com/global/article/detail/T0264349EN/the-new-bmw-5-series-sedan?language=en. [Accessed 11 May 2017].

[22] Volkswagen AG. 2017. The new Volkswagen XL1 Super Efficient Vehicle (SEV). [ONLINE] Available at: http://www.volkswagen.co.uk/about-us/futures/xl1. [Accessed 11 May 2017].

[23] Mercedes-Benz / Daimler AG. 2015. Mercedes-Benz “Concept IAA”: digital transformer.. [ONLINE] Available at: https://www.mercedes-benz.com/en/mercedes-benz/design/mercedes-benz-design/concept-cars/concept-iaa-intelligent-aerodynamic-automobile/. [Accessed 12 May 2017].

[24] Gehm R., ’Active in Aero’, SAE Magazive Feature Article, 2015 doi: 15AUTP11_01

[25] Kumar, A., Singh, A. and Regin A, F., "Study on Effect of Ground Clearance on Performance of Aerodynamic Drag Reduction Devices for Passenger Vehicle Using CFD Simulations", SAE Technical Paper 2015-26-0197, 2015, doi:10.4271/2015-26-0197.

[26] Sebben, S., Vdovin, A., "Aerodynamics of Passenger Vehicles", Class Lecture, Road Vehicle Aerodynamics VT16, Chalmers Technical University, Gothenburg, 2016.

[27] Robinette, R., "Mazda Miata CFD Generated Aerodynamic Info", Online research, 2016, [ONLINE] Avaliable at: https://robrobinette.com/S2000Aerodynamics.htm [Accessed 01 June 2017]

[28] Lennart L., Jesper M., Hakan D. and Gunnar O., "Performance of an Automotive Under-Body Diffuser Applied to a Sedan and a Wagon Vehicle", Technical Paper, 2013.

[29] Kang, S., Cho, J., Jun, S., Park, H. and Song, K., "A Study of an Active Rear Diffuser Device for Aerodynamics Drag Reduction of Automobiles", SAE International. 2012-01-0173, 2012, doi: 10.4271/2012-01-0173

[30] Hamlin, P., Broniewicz, A. and Landström, C., "7 Reduction of $CO_2$ Emissions for Energy Efficient 2020 Passenger Cars by Applying State of the Art Aerodynamics Research Techniques", FKFS Conference 2015, 2015.

[31] Daryakenari, B., Abdullah, S. and Zulkifli, R., "Reducing Vehicle Drag Force Through a Tapered Rear Side Wall", SAE Int. J. Commer. Veh. 6(2):2013, doi: 10.4271/2013-01-9020

[32] Sterken, L., Lofdahl, L., Sebben, S. and Walker, T., "Effect of Rear-End Extensions on the Aerodynamic FOrces of an SUV", SAE Technical Paper 2014-01-0602, 2014, doi: 10.4271/2014-01-0602

[33] Audi AG, 1999, Press Release [ONLINE] Avaliable at: https://www.audiworld.com/model/a2/news/091499.shtml

[34] Littlewoodd, R., Passmore, M., "The Optimization of Roof Trailing Edge Geometry of a Simple Square-Back", Technical Paper, Loughborough University, 2010 .

[35] Soares, R.F., De Souza, F.J., "The Brazilian Automotive Scenario over the Hatch 2015 Car Models: A view from Aerodynamics", Technical Paper, Federal University of Uberlandia, 2015 .

[36] Esser, M., "Standardization and Vehicle Regulation Aspect of Camera Monitor System", Technical Paper, Springer International Switzerland, 2016 .

[37] Heft. A, Indinger. T, Adams. N. (2012). Introduction of a New Realistic Generic Car Model for Aerodynamic Investigations. SAE, doi:10.4271/2012-01-0168.

[38] Andersson. B. Andersson R. Håkansson L. Mortensen M. Sudiyo R. Wachem B. (2016). Computational Fluid Dynamics for Engineers: 12th ed. Chalmers University of Technology.

[39] Ishihara, Y., Takagi, H. and Asao, K. "Aerodynamic Development of the New Developed Electric Vehicle", SAE International 2011-39-7230, 2011.

[40] Vdovin A, (2013) Investigation of Aerodynamic Resistance of Rotating Wheels on Passenger Cars. Chalmers Univeristy of Technology: Chalmers Reproservice

[41] Kounenis, C., Bonitz, S., Ljungskog, E., Sims-Williams, D. et al., "Investigations of the Rear-End Flow Structures on a Sedan Car," SAE Technical Paper 2016-01-1606, 2016, doi:10.4271/2016-01-1606.

[42] Renault Eolab Concept (2017). [ONLINE]. Available at: https://www.renault.co.uk/vehicles/concept-cars/eolab.html (2017-06-05)

# A
# Radiator Data

The radiator data calculations are based on a 2015 radiator simulation representing a generic radiator pressure drop for different vehicle speeds.

**Table A.1:** Radiator Pressure Drop Simulation Results

| 2015 Radiator Simulation | |
|---|---|
| Velocity [m/s] | Pressure Drop [Pa] |
| 3 | 59.1813 |
| 4 | 105.1796 |
| 5 | 164.3135 |
| 6 | 236.583 |
| 7 | 321.9881 |
| 8 | 420.5288 |
| 9 | 532.2051 |
| 10 | 657.017 |
| 11 | 794.9645 |
| 12 | 946.0476 |
| 13 | 1110.2663 |
| 14 | 1287.6206 |
| 15 | 1478.1105 |

Matlab is used to calculate the inertial resistance and the viscous resistance coefficient.

```
clc
clear all
close all

v = [3 4 5 6 7 8 9 10 11 12 13 14 15] ; % test velocity [m/ s]
Radiator2015_dp=[59.1813
105.1796
164.3135
236.583
321.9881
420.5288
532.2051
657.017
```

```
794.9645
946.0476
1110.2663
1287.6206
1478.1105 ] ; %test pressure drop [Pa]

radiator_thickness=0.03; % Radiator Thickness [m]
Radiator2015_dp_l=Radiator2015_dp/radiator_thickness; % [Pa/m]

% Inertial Resistance Coeff: 218.93 [kg/m^4]
% Viscous Resistance Coeff : 0.79 [kg/m^3*s]
y=(218.93*v .^2+0.79* v );

% Genarete the plot for checking the results is correct.
plot(v,Radiator2015_dp_l,'b',v,y,'r')
legend ('Data' ,'Curve Fitting')
xlabel('v[m/s]')
ylabel('dp/length [Pa/m]')
```